OPTIMIZING SH-SY5Y CELL DIFFERENTIATION INTO NEURONS AND INVESTIGATING THE EFFECTS OF FLAVONOIDS ON NEURODEGENERATION

by

Meryem Şahin

B.S., in Chemistry, Bogazici University, 2013

Submitted to the Institute of Biomedical Engineering
in partial fulfillment of the requirements
for the degree of
Master of Science
in
Biomedical Engineering

Boğaziçi University
2019

ACKNOWLEDGMENTS

I would like to dedicate this thesis to my grandfather. Seeing him live with Parkinson's Disease has been very painful. But his kind heart and continuous love, even when going through this devastating disease, have always reminded me of the things that are the most important in life.

I would like to express my deepest gratitude to my thesis supervisor Prof. Dr. Hale Saybaşılı for her guidance and patience throughout my studies. Being in her class, and then joining her laboratory to learn about neuroscience and electrophysiology was one of the greatest fortunes I have had.

I am also grateful to Assoc. Prof. Dr. Bora Garipcan as he opened his cell culture laboratory to me. In addition, I thank Alp Özgün and Fatma Zehra Erkoç for their immeasurable help with the numerous problems I have encountered about cell culture.

I also would like to thank Prof. Dr. Ayşegül Köroğlu for trusting me with Sideritis brevibracteata extracts.

I sincerely thank Gül Öncü, Murat Can Mutlu and Sefa Erdoğan for their help with the electrophysiology experiments and setup.

Lastly, I want to thank my mother and my father for their endless love and support. Their happiness with my interest in pursuing academic studies fuels me to work harder.

This thesis was partly funded by Boğaziçi University Research Fund Grant No. 13362.

ACADEMIC ETHICS AND INTEGRITY STATEMENT

I, Meryem Şahin, hereby certify that I am aware of the Academic Ethics and Integrity Policy issued by the Council of Higher Education (YÖK) and I fully acknowledge all the consequences due to its violation by plagiarism or any other way.

Name :

Signature:

Date:

ABSTRACT

OPTIMIZING SH-SY5Y CELL DIFFERENTIATION INTO NEURONS AND INVESTIGATING THE EFFECTS OF FLAVONOIDS ON NEURODEGENERATION

Parkinson's disease is the second most common neurodegenerative disease both in Turkey and in the world. The studies show the effects of inflammatory mechanisms and reactive oxygen species in the neurodegenerative diseases. In this respect, studying anti-inflammatory and antioxidant drugs on the models of Parkinson's is of great importance. *Sideritis brevibracteata* (P.H. Davis) is a plant endemic to Turkey that is being consumed by local people as tea to treat rheumatic pain, gastrointestinal tract problems and the common cold. Previous studies show the water-soluble flavonoids of the plant have antioxidant and anti-inflammatory effects. SH-SY5Y neuroblastoma cells are commonly used in the literature as neuronal models, however, there is no agreed-upon differentiation protocol to conduct reliable research. In this thesis, differentiation of SH-SY5Y cells into neurons was optimized, then Parkinson's Disease was modeled in SH-SY5Y neuroblastoma cells using rotenone. Then, *S. brevibracteata* extract was investigated to see whether or not it has an effect on these cells in terms of protection, using a cell viability assay. Results showed that 1 µg/mL *S. brevibracteata* can protect the cells against 20 µM rotenone induced toxicity.

Keywords: SH-SY5Y, electrophysiology, Western blot, Sideritis brevibracteata, , neurodegenerative diseases.

ÖZET

SH-SH5Y HÜCRELERİNİN NÖRONA FARKLILAŞTIRILMASININ OPTİMİZASYONU VE SIDERITIS BREVIBRACTEATA ÖZÜTÜNÜN NÖRODEJENERASYON İNDÜKLENMİŞ SH-SY5Y HÜCRELERİNE ETKİLERİNİN İNCELENMESİ

Parkinson Hastalığı Türkiye ve dünyada en yaygın ikinci nörodejeneratif hastalıktır. Nörodejeneratif hastalıklarda enflamatuar mekanizmaların ve reaktif oksijen türevlerinin etkili olduğu düşünülmektedir. Bu açıdan, antienflamatuar ve antioksidan ilaçların Parkinson hastalığının modellerinde incelenmesi büyük bir öneme sahiptir. *Sideritis brevibracteata* (P.H. Davis) Türkiye'ye endemik, Akdeniz Bölgesi'nde yerel halk tarafından romatizmal ağrıları, mide-bağırsak sistemi rahatsızlıklarını ve soğuk algınlığını tedavi etmek için çay olarak tüketilen bir bitkidir. Yapılan çalışmalar bitkinin özütünden elde edilen suda çözünebilen flavonoitlerin antienflamatuar ve antioksidan özelliklere sahip olduğunu göstermektedir. SH-SY5Y nöroblastoma hücreleri, literatürde sıklıkla nöron modeli olarak kullanılmaktadır, ancak henüz bu hücrelerin farklılaştırılması için üzerinde anlaşılmış bir farklılaştırma protokolü bulunmamaktadır. Bu tezde, SH-SY5Y hücrelerinin nörona farklılaştırılması optimize edilmiş, ardından hücrelerde rotenon ile Parkinson hastalığı modellenmiştir. Daha sonra, bir canlılık testi ile *S. brevibracteata* özütünün hastalık modellenmiş hücrelerde koruyucu bir etkisi olup olmadığı incelenmiştir. Sonuçlar 1 µg/mL *S. brevibracteata*'nın, 20 µM rotenon ile indüklenen toksisiteye karşı hücreleri koruduğu belirlenmiştir.

Anahtar Sözcükler: SH-SY5Y, elektrofizyoloji, Western blot, Sideritis brevibracteata, nörodejeneratif hastalıklar.

TABLE OF CONTENTS

LIST OF FIGURES

LIST OF ABBREVIATIONS

^{1}H-NMR	Proton Nuclear Magnetic Resonance
^{13}C-NMR	Carbon-13 Nuclear Magnetic Resonance
AFM	Atomic Force Microscopy
ANOVA	analysis of variance
AO/PI	acridine orange/propidium iodide
BDNF	brain-derived neurotrophic factor
BSA	bovine albumin serum
C_m	membrane capacitance
$CaCl_2$	calcium chloride
CHOL	cholesterol
CsCl	cesium chloride
DA	dopamine
DAPI	4',6-diamidino-2-phenylindole
DAQ	data acquisition
DMEM	Dulbecco's Modified Eagle's Medium
DMSO	dimethyl sulfoxide
E2	estradiol
EGTA	egtazic acid
FBS	fetal bovine serum
GAP-43	growth associated protein 43
GPX	glutathione peroxidase
HEPES	4-(2-hydroxyethyl)-1-piperazineethanesulfonic acid
IC_{50}	half maximal inhibitory concentration
IR	infrared
IV	current-voltage
K^+	potassium ion
KCl	potassium chloride
KOH	potassium hydroxide

MAP	microtubule-associated protein
$MgCl_2$	magnesium chloride
MPLC	Medium Pressure Liquid Chromatography
MS	Mass Spectrometry
MTT	3-(4,5-dimethylthiazol-2-yl)-2,5-diphenyltetrazolium bromide
Na^+	sodium ion
NaCl	sodium chloride
NaOH	sodium hydroxide
NeuN	neuronal nuclei
NGF	nerve growth factor
$NMDG^+$	N-methyl-d-glucamine
NSAID	non-steroidal anti-inflammatory drugs
PBS	phosphate buffered saline
PC12	rat pheochromocytoma cell line
PD	Parkinson's Disease
PVDF	polyvinylidene fluoride
RA	retinoic acid
RIPA	radioimmunoprecipitation assay
ROS	reactive oxygen species
SDS	sodium dodecyl sulfate
SH-SY5Y	human neuroblastoma cells
SNc	substantia nigra pars compacta
SOD	superoxide dismutase
SV2	synaptic vesicle protein 2
SYN	synaptophysin
TBS-T	tris-buffered saline with Tween 20
TMB	3,3',5,5'-tetramethylbenzidine
TPA	12-O-tetradecanoyl phorbol 13-acetate
TrkB	tyrosine receptor kinase B
TUJ1	β-tubulin

1. MOTIVATION

The progressive degeneration of the neurons in the nervous system and related functional losses in the body is called neurodegeneration. Neurodegenerative diseases affect millions of people throughout the world [1]. Even though it has been shown that the neurodegenerative diseases cause %25 of all deaths and disabilities throughout the world, effective treatments for these diseases are yet to be found [2]. To better study the possible protective and treating agents researchers are trying to find valid models *in vitro*. For the time being, the available treatments for managing these disorders are not adequate. One of the commonly used models for neurodegeneration research is SH-SY5Y human neuroblastoma cell line. However, there is no agreed-upon differentiation protocol into neurons for this cell line.

During my thesis work, my aim was to first refine the differentiation protocol of SH-SY5Y human neuroblastoma cell line through analyses with electrophysiological recordings, Western blotting, and immunocytochemistry, and then, to test Sideritis brevibracteata which is an endemic species to Turkey in terms of its protective effects against rotenone-induced neurodegeneration using differentiated SH-SY5Y cells.

2. INTRODUCTION

2.1 Differentiation of Neuroblastoma Cells into Neuron Like Cells

This section deals with the characteristics of SH-SY5Y human neuroblastoma cell line and its proper differentiation into neuron-like cells. Different applications of this cell line in modeling neurons and neurodegenerative diseases have made numerous studies possible, however, the discrepancies between the cell culture and differentiation methods have led us to think about finding the optimal method for differentiating these cells into neurons. To have a near-perfect model for neurons and study neurodegenerative diseases more accurately, defining an optimal model is essential. Here, the thought process leading to several different differentiation protocols and various analysis methods for understanding these cells more closely have been described.

2.1.1 SH-SY5Y Human Neuroblastoma Cell Line

SH-SY5Y cell line is a subclone of SK-N-SH cell line which was obtained from a 4-year-old neuroblastoma patient's bone marrow in 1970 [3]. Being cancer cells, these cells proliferate rapidly in the undifferentiated form. Undifferentiated SH-SY5Y cells grow in clusters and they have short, truncated processes and bigger cell bodies than the differentiated cells, whereas the differentiated cells have longer processes with polarized cell bodies [4]. Differentiation withdraws cells from the cell cycle so that they will be arrested in the G0 and G1 phases of the cell cycle. This will prevent cells from proliferating and the number of cells in culture conditions will not grow throughout planned experiments.

SH-SY5Y human neuroblastoma cells comprise of both adherent and floating cells. The adherent cells are the S-type epithelial-like cells, whereas the floating cells

are N-type neuroblast-like cells. Also, being human cells, they express some human-specific proteins [4], so they are more similar to human neurons than primary rodent cultures or rodent brain slices. Upon differentiation, neurites elongate and cells express mature neuron markers, such as growth associated protein (GAP-43), neuronal nuclei (NeuN), synaptophysin (SYN), microtubule-associated protein (MAP), synaptic vesicle protein 2 (SV2) [5], and β-tubulin (TUJ1) [6]. Among these markers, TUJ1 and SYN are widely used in Western blot and immunostaining studies to evaluate the effects of differentiation [7, 8].

For neuronal differentiation, many protocols have been suggested including a Vitamin A derivative all-trans retinoic acid (RA), 12-O-tetradecanoyl phorbol 13-acetate (TPA), brain-derived neurotrophic factor (BDNF), nerve growth factor (NGF), cholesterol (CHOL) and estradiol (E2) [6, 9–11]. Encinas et al. published their work on the differentiation of SH-SY5Y cells with both RA and BDNF, using RA followed by the addition of BDNF at day 5 of the differentiation. They have shown that the proliferation of S-type cells increases progressively with longer incubation times with RA. Also, they have shown that upon the addition of RA, Tyrosine receptor kinase B (TrkB) expression is induced at the maximum level on day 5, and then BDNF contributes to morphological differentiation of the cells through acting on these receptors [12].

2.1.2 Differentiation

Even though the differentiating agents and their effects are extensively analyzed to ensure a complete neuronal differentiation, the optimal concentrations for them have not been set, yet. The most common RA concentration used in literature is 10 µM [4, 6, 10]; but in a number of papers, different concentrations of RA (ranging from 1 nM to 33 µM) is being used for the same purpose [13–16]. BDNF and NGF concentrations used in studies also vary from 10 to 100 ng/mL [12, 13, 17].

In addition to RA and BDNF treatments proposed by Encinas et al., it was suggested that CHOL and E2 should also be used for differentiating the neuroblas-

toma cells to neurons [11]. Teppola et al. compared morphology and synaptic vesicle recycling differences between the different experimental groups, and outcome of their results indicated that a combination of RA and CHOL should be used to have a better neuronal model.

2.1.3 Electrophysiology

Electrophysiology studies performed on human neuroblastoma cells are not very commonly encountered in the literature. Halitzchi et al. reported the existence of outward K^+ and inward Na^+ currents in undifferentiated SH-SY5Y cells. However, they were not able to perform patch-clamp on differentiated cells since they were harder to clamp [18]. Almost all of the patch-clamp studies on differentiated SH-SY5Y cells use relatively high concentrations of RA (10 µM) [19]. Arcangeli et al. used 10 µM RA and 100 ng/mL BDNF, which makes their study the only study in the PubMed database that uses both RA and BDNF for electrophysiological investigation of SH-SY5Y cells [20].

2.1.4 Western Blotting

Western blotting is a technique that utilizes the size of the different proteins to separate them along an electric field. The technique was first described by Towbin et al. [21] and named by Burnette et al. [22]. It is considered a semi-quantitative method, so one must interpret the Western blot results in terms of comparisons among different experimental groups, instead of absolute concentrations of proteins. After proteins are separated, they are transferred onto a membrane to be probed with antibodies of interest. During my thesis work, Western blot was employed to understand the effects of different differentiation protocols on expressions of proteins TUJ1 and SYN.

2.1.5 F-actin & DAPI Imaging

Immunocytochemistry uses the specific antigen-antibody binding properties of the subcellular materials. The antibodies with fluorescent stains attached to them help visualize the proteins and other subcellular materials, *in vitro*. This visualization gives an idea about the presence and location of that antigen. For example, fluorescent conjugated phalloidin forms tight complexes with filamentous F-actin, but it does not form complexes with globular G-actin (monomer of F-actin) [23]. 4',6-diamidino-2-phenylindole (DAPI) stain fluoresces when it is bound to the nuclear DNA [24]. These stains are commonly used to visualize actin structure and nuclei of the cells.

2.2 Evaluation of the Neuroprotective Effects of Sideritis brevibracteata

This section explains Parkinson's Disease (PD) and the necessity for a neuroprotective agent against PD. Rotenone was used to model PD in SH-SY5Y human neuroblastoma cell line and Sideritis brevibracteata (P.H. Davis) was evaluated in terms of its efficacy in protecting the cells from neurodegeneration induced by rotenone.

2.2.1 Parkinson's Disease

Parkinson's Disease is characterized by motor symptoms such as resting tremors, rigidity, gait impairments and bradykinesia and non-motor symptoms such as; cognitive dysfunction, depression and sleep disorders. The second most common neurodegenerative disease after Alzheimer's Disease, PD affects 1-3% of the population over the age of 65. Pathologically, loss of dopaminergic neurons in substantia nigra pars compacta (SNc) and appearance of insoluble α-synuclein aggregations (Lewy bodies) are observed, leading to the degeneration of nigrostriatal pathway and decrease of dopamine (DA) in the brain.

The motor symptoms of PD results from the impairment of the control of the basal ganglia over motor cortex. The schematic of this control is given in Fig. 2.1. The basal ganglia act as brakes on voluntary movement. The brakes can be removed when DA is released from SNc [25]. In PD, the cortico-striatal pathway becomes degenerated and associated motor problems arise [26].

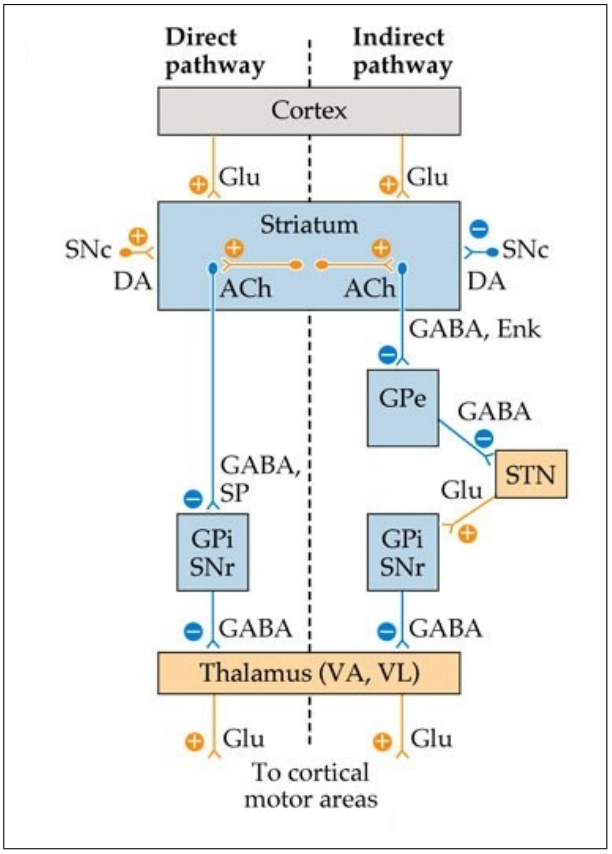

Figure 2.1 Effects of basal ganglia on movement through direct and indirect pathways. Glu: glutamate; ACh: acetylcholine; Enk: enkephaline; DA: dopamine; SNc: substantia nigra pars compacta; SNr: substantia nigra pars reticularis; GPe: globus pallidus external; GPi: globus pallidus internal; STN: subthalamic nucleus [27].

Levodopa, which is the most common medication given to PD patients, can elevate the quality of life of the patients and decrease the mortality rates during the first years of the disease onset. However, some of the symptoms of PD such as postural instability and problems with speech are not affected by this drug. And even the symptoms that improve with levodopa, become unstoppable after the tenth year of the disease onset in almost all patients [28]. After Pfizer terminated their research on Alzheimer's and Parkinson's Diseases, the challenges surrounding the treatments of diseases have become even deeper [29].

2.2.2 Preventive Approaches against Neurodegeneration

As more and more researchers point out the effectiveness of protecting the organism, before it breaks down, various studies revealed protective measures, lifestyle and diet can prevent neurodegeneration or delay the disease onset [30, 31]. In a study, 447 healthy subjects were divided into three groups [32]. The first group was asked to follow a Mediterranean diet with the requirement to have 1 L olive oil per week. The second group was asked to have a Mediterranean diet with the requirement to have 30 g nuts per day. And the third group was asked to continue with their normal diet to be the control group of the study. Four years after the start of the experiment, it was found that the cognitive functions are better in the first two groups than in the control group. Another study found Alzheimer-like brain atrophy in the brains of healthy individuals, who do not follow a Mediterranean diet [33]. Moreover, a sixteen year-long survey study with 130,000 participants revealed that Mediterranean diet lowers the risk of PD [34].

These studies call forth the question of the biological mechanisms on which Mediterranean diet acts to prevent neurodegeneration. As a possible answer, the responsible effects of Mediterranean diet may stem from high anti-inflammatory and antioxidant content of the foods that are consumed in relatively large amounts in this diet [35]. This implication is important in that the anti-inflammatory and antioxidant molecules may be evaluated as preventive medicine for neurodegenerative diseases.

2.2.3 Inflammation and Neurodegeneration

In the physiological sense, inflammation is a crucial mechanism in protecting the body from microorganisms and ensuring maintenance and repair of the tissues. Normally, inflammation steps in only when it is needed and once the problem subsides, it goes back to a quiet standby. This type of inflammation is called acute inflammation [36]. However, aging, autoimmune disorders and neurodegeneration result in chronic inflammation. When chronic inflammation cannot be stopped, outcomes may become

devastating for the organism [37]. Even though the brain does not possess all properties of peripheral inflammation, neuroinflammation is an important aspect of the brain's reaction to cellular stress and injury. The most significant indicator of neuroinflammation is the activation of astrocytes and microglia. During an inflammatory reaction, the cell bodies of these cells become more spherical, their nuclei enlarge, and their processes elongate [38].

In PD, the increased amount of cytokines shows microglia involvement in neurodegeneration which implies neuroinflammation. Also, a positive correlation was found between experiencing head trauma during the early years of life and having PD later in life, which is another indicator implying inflammatory involvement in PD [39]. SNc has a higher microglia content which makes it more vulnerable to inflammation [40].

2.2.4 Oxidative Stress and Neurodegeneration

The brain is readily susceptible to oxidative stress as a result of its high demand for energy production via aerobic respiration. In a tissue which has increased oxidative stress, the concentration of Reactive Oxygen Species (ROS) is increased. These species are molecules with a single electron in their valance shell. Having a single electron alone makes the molecules very reactive because of its need to stabilize itself by taking another electron from the environment, so that the single electron in the valance shell is paired. In biological organisms, these electrons are paired with electrons that they transfer from biological macromolecules such as nucleic acids and lipids [41]. The loss of electron causes the macromolecules to change their conformation and thus, lose their function. In a healthy organism, the produced ROS are used in cellular signaling mechanisms and then, they are stabilized by enzymatic and non-enzymatic antioxidants. If these mechanisms fail or the production becomes too much for the antioxidants to stabilize, ROS start accumulating. As they stabilize themselves, they will disrupt the physiological functioning of the cells by breaking down the aforementioned macromolecules. This process may result in cancer or apoptosis [42, 43].

Electron transport chain in mitochondria is the site where the most ROS are produced [44]. The activity of electron transport chain site Complex I is decreased in PD patients. Due to the lower Complex I activity, O_2 takes up only one electron and become partially reduced to $O_2^{\bullet}$, leading to the generation of a hydroxyl radical $OH^{\bullet}$ [26].

$OH^{\bullet}$ is the most dangerous radical for the organism. Some of the reactions that produce hydroxyl radical are given below. Reaction (2.1) shows ionization of a water molecule by radiation, (2.2) shows the reaction of H_2O_2 with iron or copper, (2.3) shows decomposition of peroxynitrite and (2.4) shows the reaction of ozone with phenols [45].

$$H_2O \longrightarrow H^{\bullet} + OH^{\bullet} \tag{2.1}$$

$$H_2O_2 + Fe^{2+} \text{ or } Cu^{2+} \longrightarrow OH^{\bullet} + OH^{-} + Fe^{3+} \text{ or } Cu^{3+} \tag{2.2}$$

$$HONOO \longrightarrow OH^{\bullet} + NO_2^{\bullet} \tag{2.3}$$

$$PH + O_3 \longrightarrow OH^{\bullet} + P + O_2 \tag{2.4}$$

In above reactions, it can be seen that the presence of excess iron may induce the conversion of H_2O_2 into $OH^{\bullet}$ which is a much more unstable ROS. As iron is necessary for oxygen transportation and neurotransmitter and myelin synthesis, it can be found abundantly throughout the nervous system which makes brain more susceptible to oxidative stress [46]. Brain's high energy demand and high concentration of iron make antioxidants crucial for healthy functioning of the brain.

Antioxidants are defined to be "any substance that delays, prevents, or removes oxidative damage to a target molecule" [47]. There are two types of antioxidant systems in the body: antioxidant enzymes and non-enzymatic small molecule antioxidants. Enzymes such as superoxide dismutase (SOD) and glutathione peroxidase (GPX) stabilize more reactive ROS into less reactive H_2O_2, and catalase turns H_2O_2 into water and oxygen [48]. H_2O_2 metabolism mostly takes place within peroxisomes to avoid damage to essential cellular structures. Aside from the enzymes, there are non-enzymatic antioxidants which can be grouped as metabolic and nutritional antioxidants [43]. These substances receive the extra electron from the radicals to make them stable. With this

extra electron they become unstable themselves, but since their energy is lower than the ROS, they do not harm the organism. The one caveat is the fact that once they received that electron, they can no longer act as an electron acceptor. This is why a constant supply of non-enzymatic antioxidants is necessary for the organism.

Effectiveness of the antioxidant mechanisms such as SOD, GPX and catalase decline with age, which is thought to play a role in the positive correlation of age with neurodegenerative diseases [49]. It was observed that the activity of Complex I protein in electron transfer chain of PD patients is lower than that of the healthy individuals. In light of this finding, it was suggested that the death of the dopaminergic neurons in SNc may be a result of increased oxidative stress stemming from the decrease of the Complex I activity which implies the role of oxidative stress in PD pathology.[48].

2.2.5 Anti-inflammatory and Antioxidant Drugs for Neurodegeneration

Inflammatory mechanisms and oxidative stress are influential both for the occurrence and in the destructive results of neurodegenerative diseases. As the hopes for finding new drugs to treat neurodegeneration, it becomes more and more important to study the effects of anti-inflammatory and antioxidant drugs on the prevention and treatment of neurodegeneration. Epidemiological studies showed that usage of non-steroidal anti-inflammatory drugs (NSAID) for long periods decreased the risk of neurodegeneration compared to the people who do not use NSAIDs [50]. Another study showed that the antioxidant Vitamin E decreased the Amyloid beta induced cell death in rat pheochromocytoma PC12 cell line [51]. It was also found that Vitamin C lowers the effect of neurodegeneration in rats [52]. When these vitamins were used in combination, they can decrease the effects of neurodegeneration in humans [53].

These promising suggestions could not be further tested in large scale controlled experiments because of the gastrointestinal and cardiovascular side effects of the NSAIDs [50]. Thus, the search of natural products which can give the same effects as those drugs without the side effects has increased. In this sense, especially

flavonoids which are a subgroup of polyphenols have gained popularity since the early 2000s. Availability of these substances through food and drinks may explain the interest towards them in the literature [54]. From the studies showing that some flavonoids can pass through blood-brain barrier [55] and that flavonoid rich foods enhance the cognitive function and prevents neurodegenerative disorders show that flavonoids should be scrutinized in the laboratories [56].

2.2.6 Sideritis brevibracteata

Sideritis brevibracteata (P.H. Davis) or locally "Alanya Adaçayı" is a plant endemic to Turkey. *S. brevibracteata* was proven to have the highest antioxidant effect among the Sideritis species [57]. This finding was evaluated more closely when six different flavonoids purified from n-butanol extract of *S. brevibracteata* were tested for their anti-inflammatory and antioxidant activities [58]. In this study, Medium Pressure Liquid Chromatography (MPLC) was used to separate the flavonoids from each other. In MPLC, 2.72 g of the n-butanol extract was separated as fractions of (**1**) 88 mg, (**2**) 142 mg, (**3**) 13 mg, (**4**) 292 mg, (**5**) 118 mg, and (**6**) 44 mg. Separated flavonoids were characterized using Proton and Carbon-13 Nuclear Magnetic Resonance (^{1}H-NMR, ^{13}C-NMR), Mass Spectrometry (MS), Infrared (IR) and Ultraviolet (UV) spectrometry techniques. The names of these six flavonoids are given below and the chemical structures and percent concentrations of each flavonoids within the extract of the compounds are given in Figure 2.2.

1) Hypolaetin 7-O-[6'''-O-acetyl-β-D-allopyranosyl-(1 → 2)]-β-D-glucopyranoside

2) Isoscutellarein 7-O-[6'''-O-acetyl-β-D-allopyranosyl-(1 → 2)]-β-D-glucopyranoside

3) 3'-hydroxy-4'-O-methylisoscutellarein 7-O-[6'''-O-acetyl-β-D-allopyranosyl-(1 → 2)]-β-D-glucopyranoside

4) Hypolaetin 7-O-[6'''-O-acetyl-β-D-allopyranosyl-(1 → 2)]-6''-O-acetyl-β-D-glucopyranoside

5) Isoscutellarein 7-O-[6'''-O-acetyl-β-D-allopyranosyl-(1 → 2)]-6''-O-acetyl-β-D-glucopyranoside

6) 3'-hydroxy-4'-O-methylisoscutellarein 7-O-[6'''-O-acetyl-β-D-allopyranosyl-(1 → 2)]-6''-O-acetyl-β-D-glucopyranoside

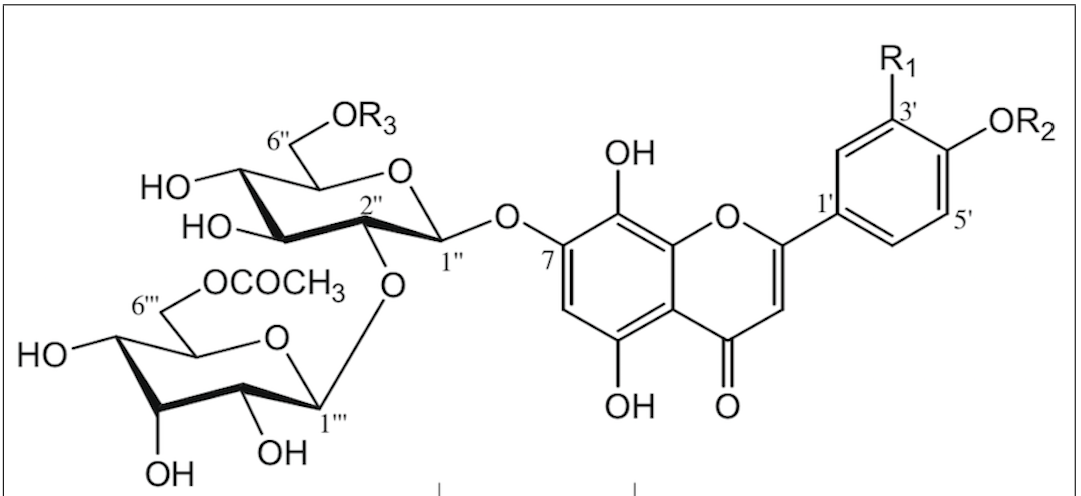

	R1	R2	R3	Percentage
1	OH	H	H	3.24
2	H	H	H	5.22
3	OH	Me	H	0.48
4	OH	H	Ac	10.74
5	H	H	Ac	4.34
6	OH	Me	Ac	1.62
TOTAL				25.64

Figure 2.2 Chemical structures of the flavonoids that are purified from the n-butanol extract of *Sideritis brevibracteata* and their percent concentrations within the extract.

Güvenç et al. have investigated above flavonoids for their antioxidant activities and found that these six flavonoids have IC_{50} values of 0.57 and 3.48 µg/mL via 1,1-diphenyl-2-picryl hydrazyl (DPPH) test [58]. These IC_{50} values were used to select three different concentrations of *S. brevibracteata*. The selected concentrations were 1, 5 and 10 µg/mL. Also, they have found that the n-butanol extract as a whole exhibited the highest anti-inflammatory activity with 26.9% to 43.8% inhibition. Being anti-inflammatory and antioxidant, *S. brevibracteata* n-butanol extract and the flavonoids can be assumed to be effective against neurodegeneration which is related to chronic

inflammation and oxidative stress [59]. However, to the best of my knowledge, *S. brevibracteata* have never been evaluated in terms of its effects of neurons.

Prof. Dr. Ayşegül Köroğlu from Ankara University and Afyonkarahisar University of Health Sciences have generously provided us with n-butanol extract of *S. brevibracteata* in its lyophilized form to ensure its stability. During my thesis studies, I have evaluated the protective effects of the n-butanol extract of *S. brevibracteata* on rotenone treated SH-SY5Y human neuroblastoma cells via a cell viability assay.

2.2.7 Rotenone

Rotenone is widely used to model PD *in vivo* and *in vitro*. It is extracted from tropical plants, and used as insect and fish poison. Since rotenone is highly lipophilic it can reach the brain easily, passing through the blood-brain barrier. Inside the brain, it will accumulate and act as a Complex I blocker. This accumulation results in high oxidative stress and leads to neuronal death [60]. *In vivo* rotenone models of PD showed bradykinesia and postural abnormalities, and also neuronal death in SNc and appearance of Lewy bodies. The selective death of SNc neurons in the presence of rotenone shows the high sensitivity of these neurons to Complex I inhibition [26].

2.2.8 Cell Viability Tests

MTT assay and AO/PI staining are two of the widely used cell viability tests and in this thesis, these tests were employed to understand the protective effect of *S. brevibracteata* against rotenone-induced PD model of differentiated SH-SY5Y human neuroblastoma cells.

2.2.9 MTT Assay

3-(4,5-dimethylthiazol-2-yl)-2,5-diphenyltetrazolium bromide (MTT) assay is a colorimetric cell viability test developed in 1983 [61]. MTT is reduced in the mitochondria and other parts of the cells [62]. Live cells can reduce the tetrazolium salt into formazan crystals, whereas dead cells cannot. MTT test uses this exclusivity to help visualize the amount of living cells in a cell culture well. After the formed formazan crystals are dissolved and the absorbance value is read, the ratio of this absorbance and the absorbance of the control gives the percentage of the living cells compared to the control.

2.2.10 AO/PI Staining

Acridine orange and propidium iodide (AO/PI) staining is another cell viability analysis method. AO can readily enter all cells and bind with nucleic acids, however, PI is a membrane impermeable stain which can only enter the cells via large pores that are opened during cell death. Upon entering the apoptotic cells, PI binds to nucleic acids as well [63]. Under the blue filter (excitation 450 nm - emission 490 nm) AO gives green fluorescence and PI gives orange fluorescence. Under the green filter (excitation 515 nm - emission 560 nm) PI fluoresces red, whereas AO becomes almost invisible.

3. MATERIALS AND METHODS

3.1 Differentiation of Neuroblastoma Cells into Neuron Like Cells

In this section, the differentiation protocols and electrophysiological and biochemical analyses of the undifferentiated and differentiated human neuroblastoma cells are given.

3.1.1 Cell Culture and Differentiation

SH-SY5Y cell line was kindly provided by Dr. B. Garipcan (Institute of Biomedical Engineering, Boğaziçi University). Cells were cultured according to the literature with some changes in the concentrations of RA and BDNF [10, 18]. Briefly, cells were grown using Dulbecco's Modified Eagle's Medium (DMEM) and Ham's F12 supplemented with 10% Fetal Bovine Serum (FBS) and 1% penicillin/streptomycin (Biosera, France). Cells were seeded at 3 x 10^4 cells onto 14 mm cover glasses in 24 well plates and incubated at 37 °C. 24 hours after seeding, media were replaced with differentiation media. RA, E2 (dissolved in dimethyl sulfoxide (DMSO)) and CHOL (dissolved in absolute ethanol) were added to media (Sigma-Aldrich). Differentiation media also contained 1% FBS. Five days after the addition of these differentiating agents, media were replaced with serum-free medium that contains 10 ng/mL BDNF. After 48 hours, differentiated cells were ready to use for the experiments for 3-4 days.

Throughout the study, experimental groups were as the following: undifferentiated (UNDIFF); 1 µM RA differentiated (RA); 1 µM RA & 10 ng/mL BDNF differentiated (RB); 1 µM RA, 5 µg/mL CHOL, 1 nM E2 & 10 ng/mL BDNF (RBCE) differentiated. Solvents of RA, E2 (DMSO) and CHOL (ethanol) was added to each group to ensure having the same concentration of these toxic vehicles in each well to

eliminate their effect from the future analyses. Final DMSO concentration was 0.02% ethanol concentration was 0.1% in all wells. Schematic of the differentiation timeline is given in Figure 3.1

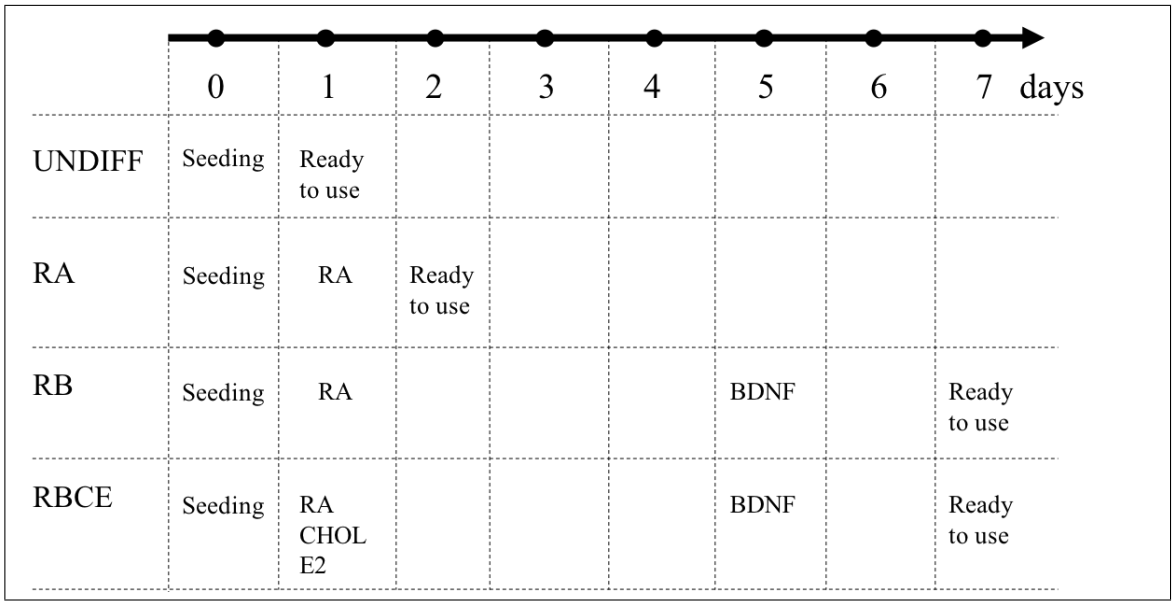

Figure 3.1 Timeline of differentiation protocols for all four experimental groups.

3.1.2 Electrophysiology

Electrophysiological activities of the cells were recorded under whole cell patch-clamp conditions [64] using AXOCLAMP 2B patch-clamp amplifier (Molecular Devices, USA) at room temperature. Electrophysiology setup was on an anti-vibration table (Newport Corp., USA) with a Faraday cage placed around the table. Data acquisition was done using ITC-18 DAQ board (Heka Instruments, Germany) and the software WinWCP (Version 5.4.1, Strathclyde University, UK). Imaging of the patch-clamp process was done using a PCO Sensicam camera (PCO Imaging Inc., Germany) and WinFluor imaging software (Version 3.2.23, Strathclyde University, UK). All signals were low-pass filtered at 1 kHz and the sampling frequency was 50 kHz. Electrophysiology setup and related electronical devices are given in 3.2

Throughout the experiments, borosilicate microelectrodes used had 3-5 MΩ resistances. The intracellular pipette solution (in mM): 4 NaCl, 140 KCl, 2 $MgCl_2$, 10

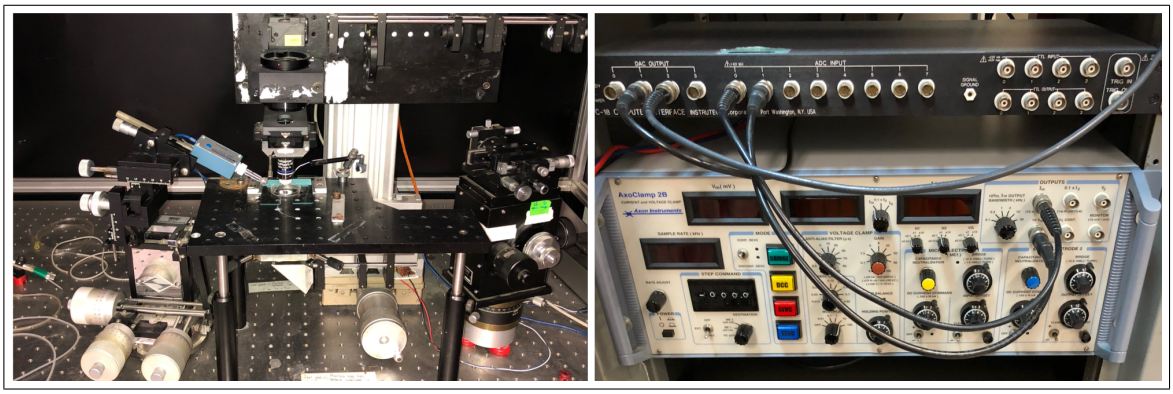

Figure 3.2 Electrophysiology setup (left), and analog-to-digital converter (top-right) and patch-clamp amplifier (bottom-right).

HEPES, 0.8 EGTA; extracellular solution (in mM): 125 NaCl, 4 KCl, 1 $MgCl_2$, 10 HEPES. 2 mM $CaCl_2$ and 10 mM glucose were added to the external solutions just before each experiment. All chemicals were purchased from Sigma-Aldrich or Merck. Extracellular solution had a pH of 7.4, which was adjusted with NaOH, intracellular solution had a pH of 7.2 which was adjusted with KOH.

Experiments were performed on relatively smaller cells to sustain better voltage-clamp conditions and to have lower membrane capacitances (C_m). The leaky recordings i.e. recordings with holding currents larger than 80 pA and recordings where series resistance was more than 15 MΩ were discarded from further analysis, hence series resistance compensation was not needed. However, capacitive transient cancellation was performed before each recording using capacitive transient cancellation knob on the front panel of the patch-clamp amplifier. After the seal is ruptured, recordings were repeated at least eight times from each cell, to ensure the stability of the seal and to be able to average the recordings to get rid of any possible oscillations.

3.1.3 Electrophysiological data analysis

The data analysis was performed via a MATLAB script (Version 2018a, Mathworks Inc., MA, USA). The script was used to, first, open the data with the .wcp file extension, convert the data to double type so that MATLAB can handle it. When

there is a different number of data points in any one of the recordings, linear interpolation was used to make sure the sizes of the data matrices were the same as each other. The script was able to plot graphs of recordings from a single cell, and to take the mean values of the currents from recordings from different cells in response to the same voltages to plot current-voltage (IV) curves.

3.1.4 Western Blot

Cells were differentiated in four groups as it was explained in Section 3.1.1. After they became ready to use, they were washed with phosphate buffered saline (PBS) and lysed with radioimmunoprecipitation assay (RIPA) buffer on ice. After centrifuging the solubilized cells at 10,000x g for 20 min the supernatant was collected. Estimation of protein concentrations was done by measuring absorbance at 280 nm. Protein samples were heated at 90 °C for 5 min and 50 µg protein per well were loaded onto a 10% sodium dodecyl sulfate (SDS)-polyacrylamide gel for resolving. After electrophoresis, the proteins were transferred to polyvinylidene fluoride (PVDF) membranes (Trans-Blot Turbo semi-dry system, Bio-rad). After the transfer, membranes were blocked with 5% fat-free milk in Tris-buffered saline with 0.1% Tween 20 (TBS-T) at room temperature for 1 h. Then, primary antibodies for target proteins TUJ1 (sc80005, Santa Cruz) and SYN (ab8049, Abcam) were applied to the membranes in 1:1000 and 1:500 dilution, respectively. The membranes were incubated overnight at 4 °C. After washing the membranes with TBS-T, the corresponding secondary antibody (ab6789, Abcam) was applied to the membranes and the membranes were kept on the shaker for 1h at room temperature. After washing membranes with TBS-T, bands were visualized with a colorimetric TMB substrate (1-step ultra 3,3',5,5'-tetramethylbenzidine (TMB) blotting solution, Thermo Fisher). Scanned membrane images were processed using ImageJ (Version 1.8.0, NIH, USA). Sequentially probed actin bands were used as the loading control. Five biological replicates were performed for TUJ1 and four biological replicates were performed for SYN.

3.1.5 F-actin & DAPI Imaging

Cells were differentiated in four groups with four wells in each group (Section 3.1.1). After they became ready to use, they were first fixed with paraformaldehyde (PFA), then permeabilized with Triton X to facilitate the binding of the antibodies to the target antigens. Followingly, they were blocked with bovine albumin serum (BSA) to prevent non-specific binding of the antibodies. The procedure is shown in Fig. 3.3. The used solutions were 4% PFA in PBS, 0.1% Triton X in PBS and 1% BSA in PBS with 0.1% Tween 20.

For staining, phallotoxin solution previously dissolved in methanol was diluted with 1% BSA to have 25 µL per mL of BSA solution. Enough solution to cover the cells (300 µL in this case) was added onto the cells. Plate was shaken on the gentle shaker for 20 minutes in the dark. The cells were checked under the blue excitation filter before discarding the staining solution, to see whether F-actin filaments are visible. When the filaments became visible staining solution was discarded and the cells were washed twice with PBS.

DAPI staining is done as the last step. 2.1 µL DAPI stain previously dissolved in methanol is diluted in 100 µL PBS. Then, it is diluted 1:1000 in PBS. Enough solution to cover the cells (300 µL) was added onto the cells. The plate was shaken on the gentle shaker for 3 minutes. Both staining solutions were used at room temperature, and the discarded solutions were kept at -20 °C for future stainings.

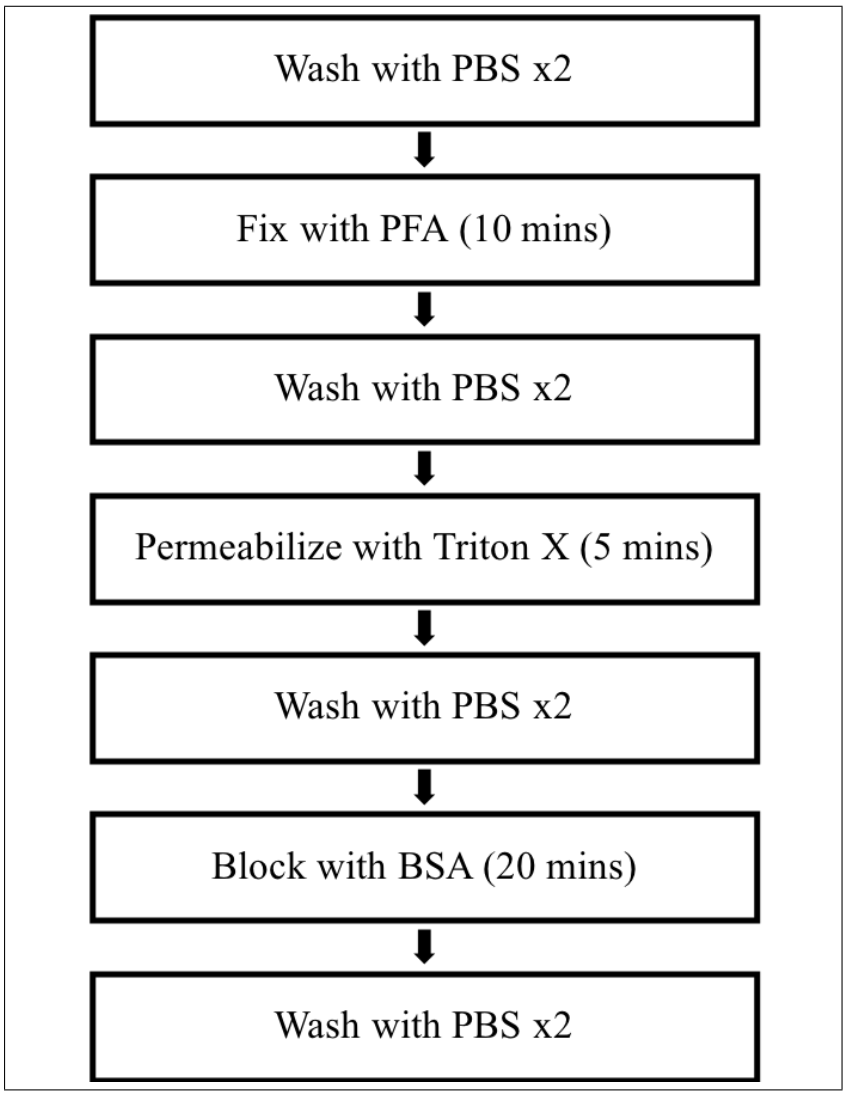

Figure 3.3 Steps of preparation of the cells for F-actin & DAPI staining.

After the images were collected, number of cells in each of ten images collected from all of the experimental groups was counted using ImageJ (Version 1.8.0, NIH, USA). These numbers were compared in order to understand the cell viability with different differentiation methods.

3.2 Evaluation of the Neuroprotective Effects of Sideritis brevibracteata

In this section, the methods for investigating the effects of *S. brevibracteata* in protecting the SH-SY5Y human neuroblastoma cells from rotenone-induced neurodegeneration is explained. Cell viabilities for different concentrations of rotenone and *S. brevibracteata* was evaluated and the results of the protective effects of *S. brevibracteata* was investigated by comparing the results of all experiments.

3.2.1 Electrophysiology

For the evaluation of the toxic effects of rotenone, 3 x 10^4 cells were seeded onto 14 mm cover glasses placed in 24-well plates in five replicate wells for each group. Differentiation protocol was the same as the protocol found to be most effective for the differentiation into neurons (i.e. 1 µM RA for 5 days followed by 10 ng/mL BDNF for 2 days).

When the differentiation was completed, rotenone was added onto the cells at 0.2, 0.5, 1 and 2 nM concentrations, one hour prior to the electrophysiological recordings. Control group had only 0.02% DMSO added, which is the amount of the highest DMSO required for dissolving rotenone.

3.2.2 Cell Viability Tests

Cell viability tests were performed to evaluate the concentration-dependent effects of rotenone and *S. brevibracteata*, and to investigate the protective effects of *S. brevibracteata* against rotenone, with determined concentrations. After 48 hours of BDNF treatment, BDNF containing serum-free media was removed and rotenone containing serum-free media was added in different concentrations for 24 hours.

3.2.2.1 MTT Assay. For the MTT assay, 5 x 10^4 cells were seeded on a 48-well plate and the cells were differentiated using the determined differentiation method (i.e. 1 µM RA for 5 days followed by 10 ng/mL BDNF for 2 days). 5, 10, 20, 100, 200 and 500 nM rotenone was added one hour prior to the MTT assay. The assay was performed in the dark. 5mg/mL MTT stock solution was prepared in PBS. Prepared solution was filtered using a filter with pore size 0.22 µm. MTT stock is diluted to have 10% v/v of MTT in medium the cell culture medium. For 48-well plate, 30 µL of MTT stock was diluted in 270 µL cell culture medium. The old cell culture medium was removed from the wells and the freshly prepared 10% MTT solution was added to the wells. The plate was incubated at the incubator for 4 hours. After 4 hours, the medium containing MTT was removed from the wells and 100 µL of DMSO was added to dissolve the formazan crystals formed. Plate was kept on the gentle shaker for 5 minutes. Absorbance of each well was read at 570 nm with the reference absorbance at 740 nm using the microplate reader (iMark, Bio-Rad).

3.2.2.2 AO/PI Staining. For the AO/PI staining, 2 x 10^4 cells were seeded on a 48-well plate and the cells were differentiated using the determined differentiation method (i.e. 1 µM RA for 5 days followed by 10 ng/mL BDNF for 2 days). Concentrations tested for rotenone was 20 and 50 µM with 12 and 24 hours application time. S. brevibracteata was added at concentrations of 1, 5 and 10 µg/mL. These concentrations were selected according to the determined antioxidant IC_{50} values by Güvenç et al. [58]. Cells were preincubated with *S. brevibracteata* for 48 hours be-

fore the rotenone application and rotenone was added 24 hours prior to the imaging. Rotenone was added to the cells in combination with fresh *S. brevibracteata*. Control group had only 0.02% DMSO added which is the amount of the highest DMSO needed for dissolving rotenone. Each group had three wells and four images were collected from each cell. Each image covers an area of about 1.1 mm^2.

5 mg/mL AO and 3 mg/mL PI solutions were prepared in absolute ethanol. For the staining solution, 1 µL from each dye solution was mixed in per mL of PBS. The medium was removed from the wells to be stained and 100 µL from the staining solution was added to each well. The plate was shaken gently for 1 minute. After 1 minute, the wells were washed with 100 µL of PBS. 100 µL of PBS was added after washing. Cells were imaged under the green filter which shows all cells green. Dead cells will be orange under the same filter and they should appear red under the blue filter. After the images were collected, ImageJ (Version 1.8.0, NIH, USA) was used to count the cells.

3.3 Statistical Analyses

Statistical analysis was performed using SPSS (Version 25, IBM, USA). For all the data, first, outliers were eliminated according to the graphical representations of the data produced by SPSS. Then, Shapiro-Wilk normality analysis was performed to decide whether to use a parametric or non-parametric test. For normally distributed Western blot, MTT and AO/PI data, one-way ANOVA followed by Tukey multiple comparisons test was performed and $p < 0.05$ was considered statistically significant. All values are given as means ± standard deviations. For electrophysiology data, no statistical test was applied as the sample sizes were not enough for statistical analysis. Throughout the results, n represents the number of samples.

4. RESULTS

4.1 Differentiation of Neuroblastoma Cells into Neuron Like Cells

4.1.1 Electrophysiology

Voltage clamp experiments were performed on each experimental group described in Section 2.1. Sample sizes were six for undiff, one for RA, three for RB and one for RBCE. Holding potential was selected to be -90 mV according to the literature [19]. Depolarizing voltages were applied as 15 steps of 10 mV pulses. Exemplary recordings of four experimental groups are given in Figure 4.1 - 4.4.

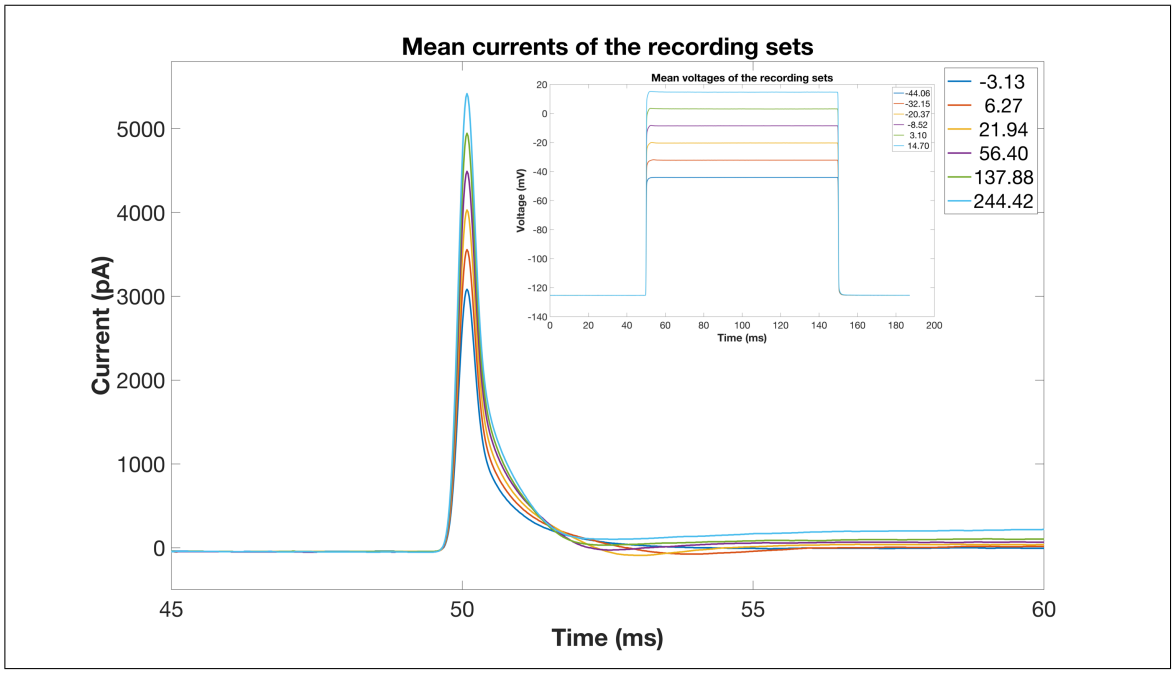

Figure 4.1 Exemplary electrophysiological voltage-clamp recordings of an undifferentiated cell where the voltages given in top right show applied voltage steps.

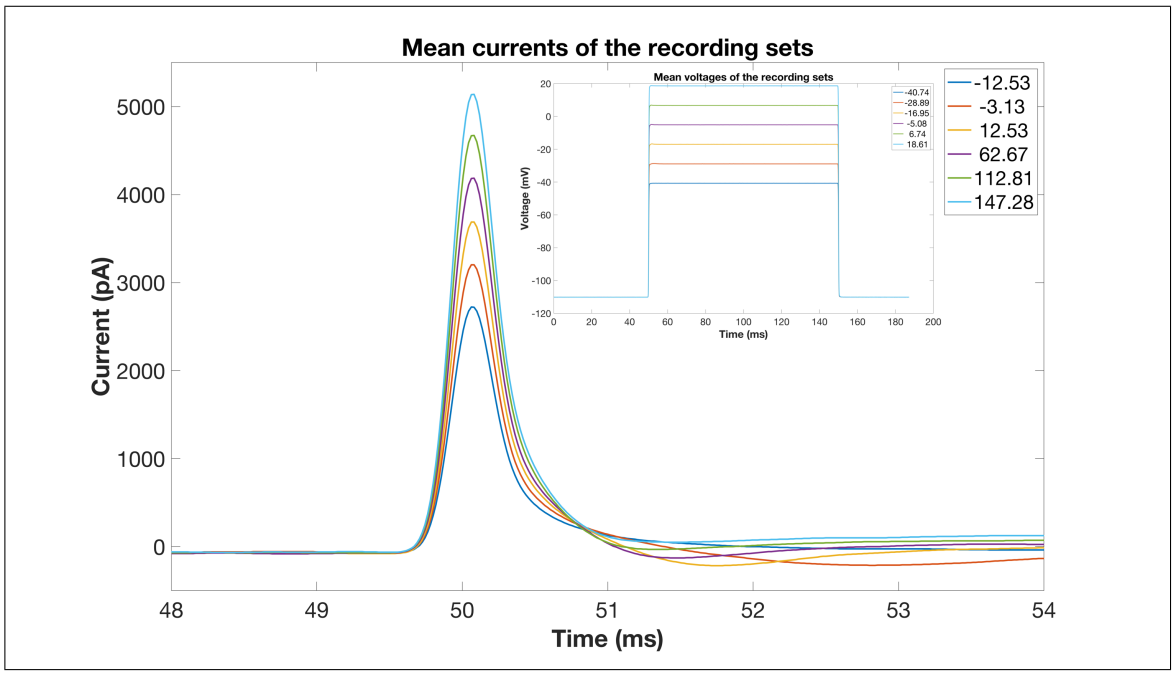

Figure 4.2 Exemplary electrophysiological voltage-clamp recordings of an RA differentiated cell.

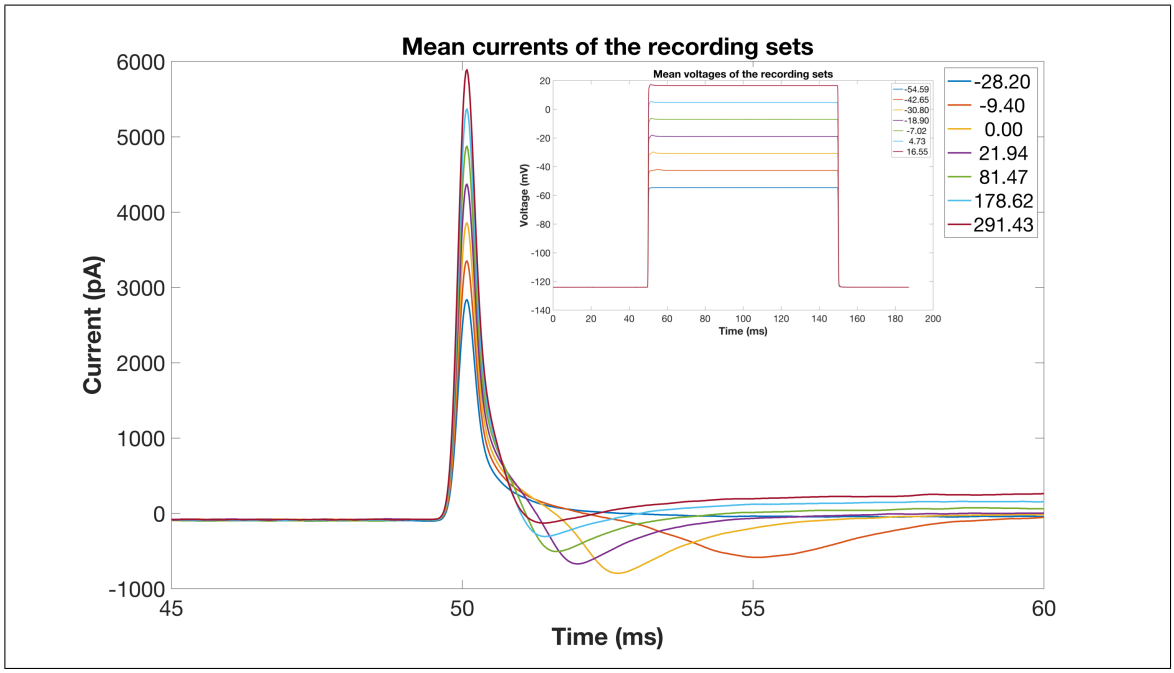

Figure 4.3 Exemplary electrophysiological voltage-clamp recordings of an RA and BDNF differentiated cell.

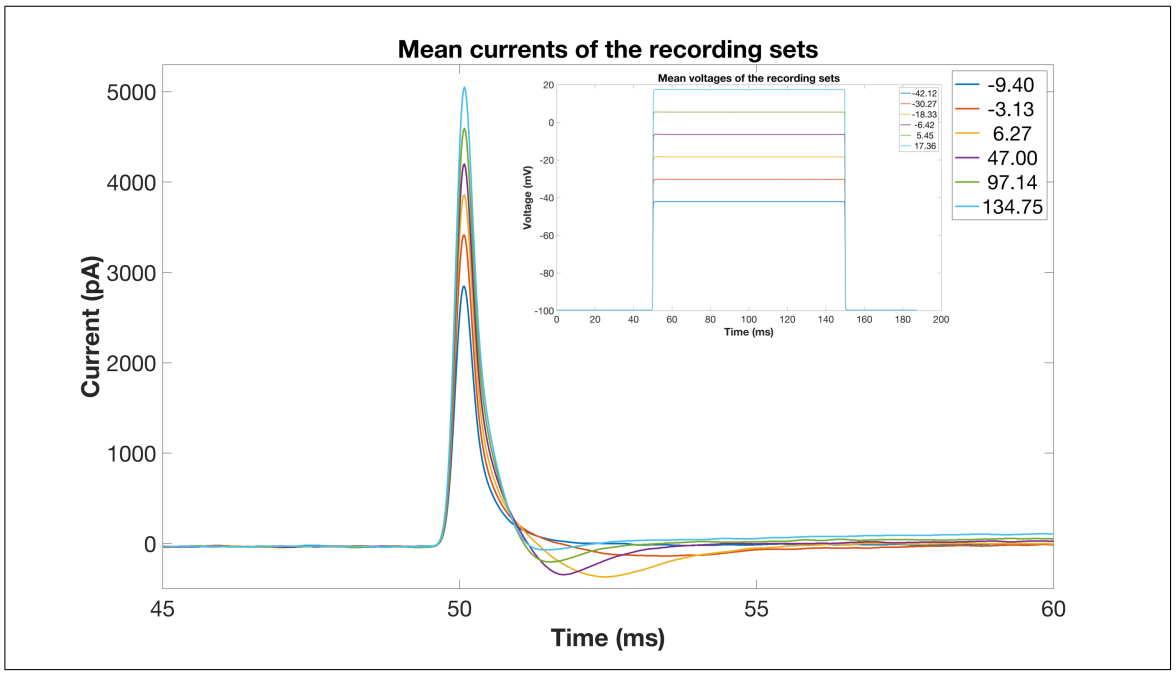

Figure 4.4 Exemplary electrophysiological voltage-clamp recordings of an RA, CHOL, E2 and BDNF differentiated cell.

Electrophysiological recordings were further examined using current voltage (IV) curves. Since only the small cells were patched membrane capacitances (Cm) were in the range of 10 pF. Hence, the IV graphs throughout this paper are given as (mV, pA) instead of (mV, pA/pF). Overall IV curves given in Figure 4.5 showed that the undifferentiated cells (n=6) can continue responding at voltages where differentiated cells cannot respond. Also, they show that undifferentiated cells produce much larger outward currents (350 pA at 50 mV), compared to the other experimental groups (180 pA at 50 mV).

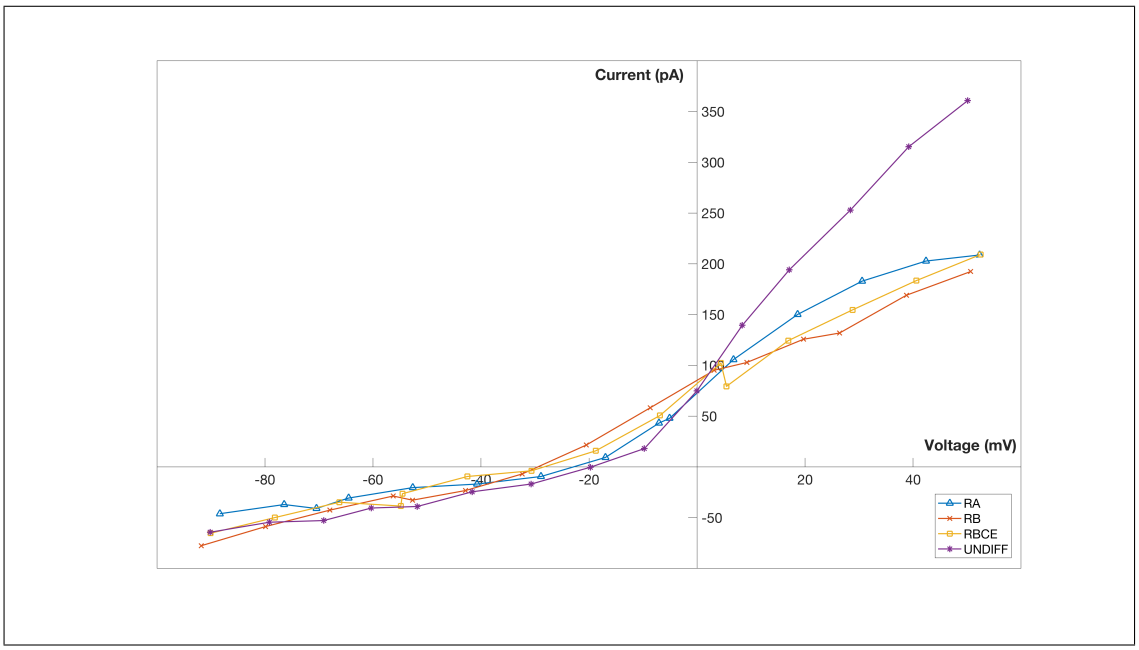

Figure 4.5 Overall current-voltage curve collected from cells that are voltage-clamped starting from -90 mV and increasing in 15 steps as 10 mV voltage steps.

IV curves where only the inward currents from each group were depicted were given in Figure 4.6. They imply the higher excitability of RB cells (n=3) compared to the other three group. RB group can produce its highest inward currents at around -38 mV, whereas other groups produce their highest inward currents between -20 and -6 mV. Undiff cells elicited minimal inward currents (50 pA) starting from around -20 mV.

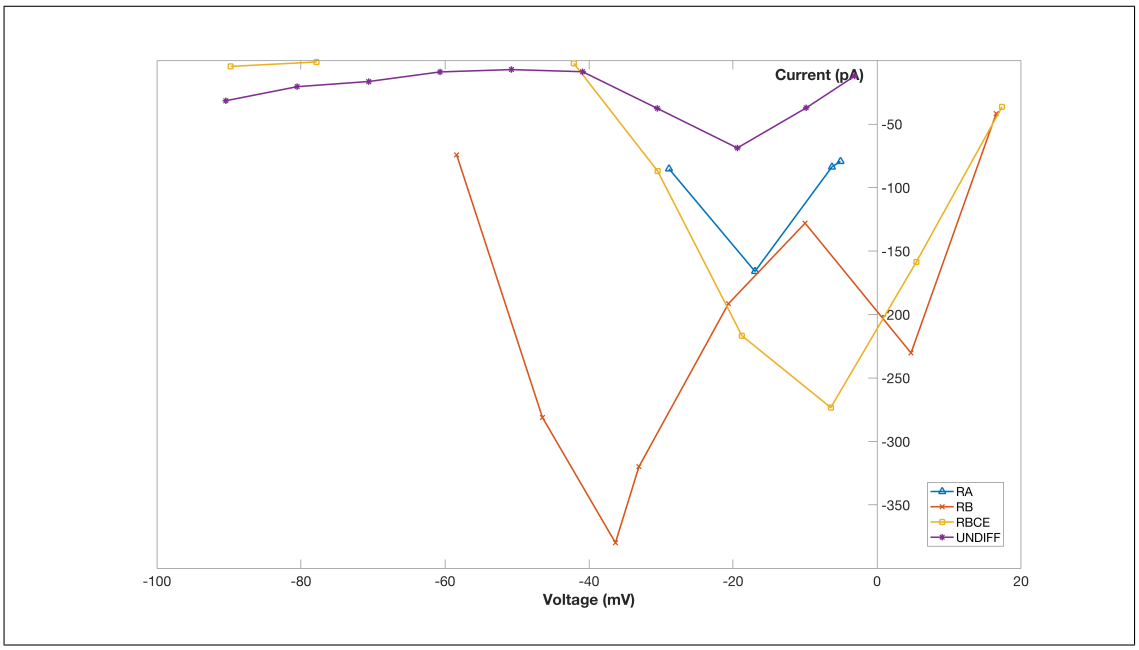

Figure 4.6 Inward current-voltage curve collected from cells that are voltage-clamped starting from -90 mV and increasing in 15 steps as 10 mV voltage steps. This graph shows only the inward current responses.

Outward currents (Figure 4.7) of the undifferentiated cells were found to be highest (300 pA) among the experimental groups.

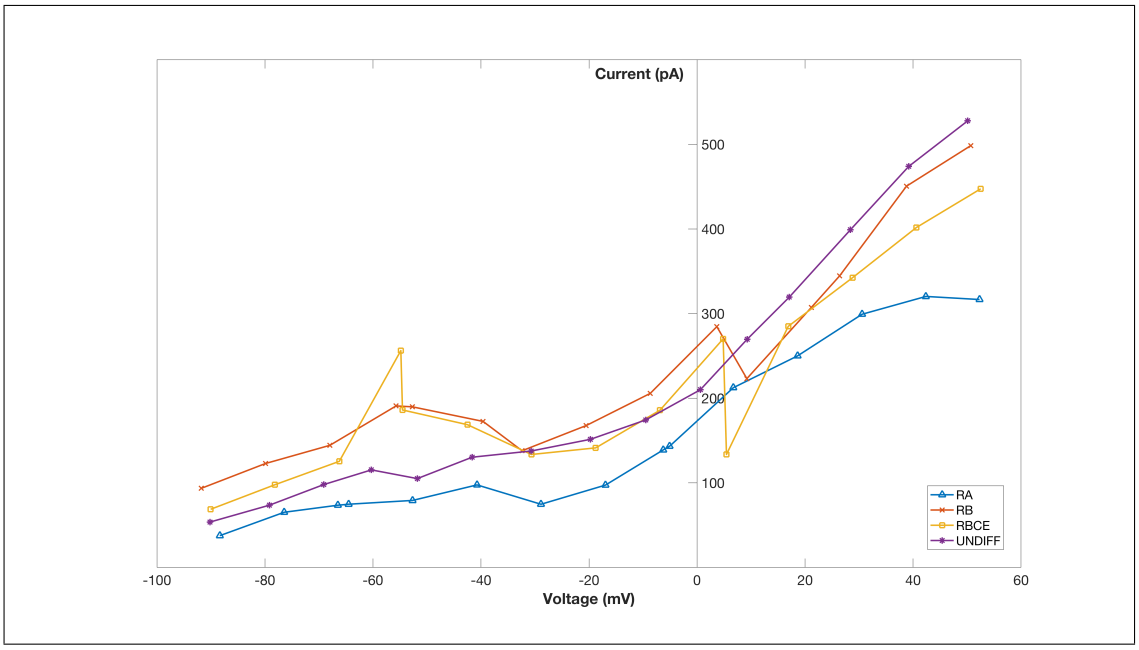

Figure 4.7 Outward current-voltage curve collected from cells that are voltage-clamped starting from -90 mV and increasing in 15 steps as 10 mV voltage steps. This graph shows only the outward current responses.

4.1.2 Western Blot

Evaluation of neuron-specific protein expressions was carried out to have an understanding of biochemical changes upon neuronal differentiation. Effects of different differentiation protocols on the expression levels of the selected proteins (TUJ1, SYN) was measured with Western blotting on five and four biological replicates, respectively. The results are given in Figure 4.8.

TUJ1 expression was found to be statistically significantly increased in RB and RBCE groups compared with the UNDIFF group ($p < 0.05$). The results of differentiation with RA did not show a statistically significant change in the expression of TUJ1. On the other hand, SYN expression was decreased with any differentiation method used compared with the undifferentiated cells ($p < 0.05$). However, when comparing the effects of various differentiation methods on SYN expression, RBCE group showed a higher expression of SYN protein than the RA group ($p < 0.05$).

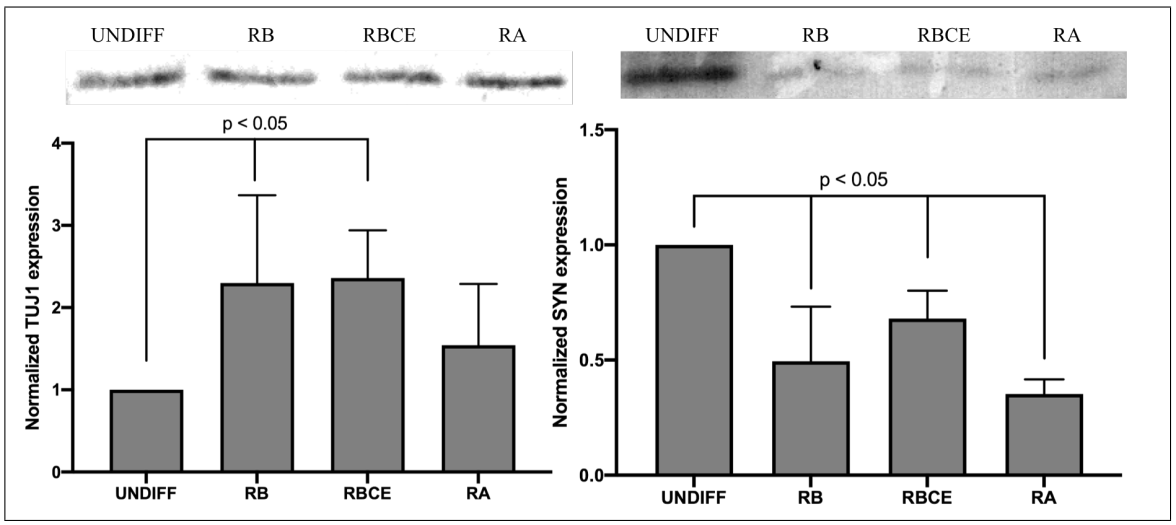

Figure 4.8 Exemplary western blots (upper panels) and normalized protein expression graphs (lower panels) for the proteins TUJ1 and SYN.

4.1.3 F-actin & DAPI Imaging

F-actin & DAPI Imaging was successfully completed, the images collected from the samples are given below as merged images of F-actin and DAPI fluorescence (Figure 4.9, Figure 4.10).

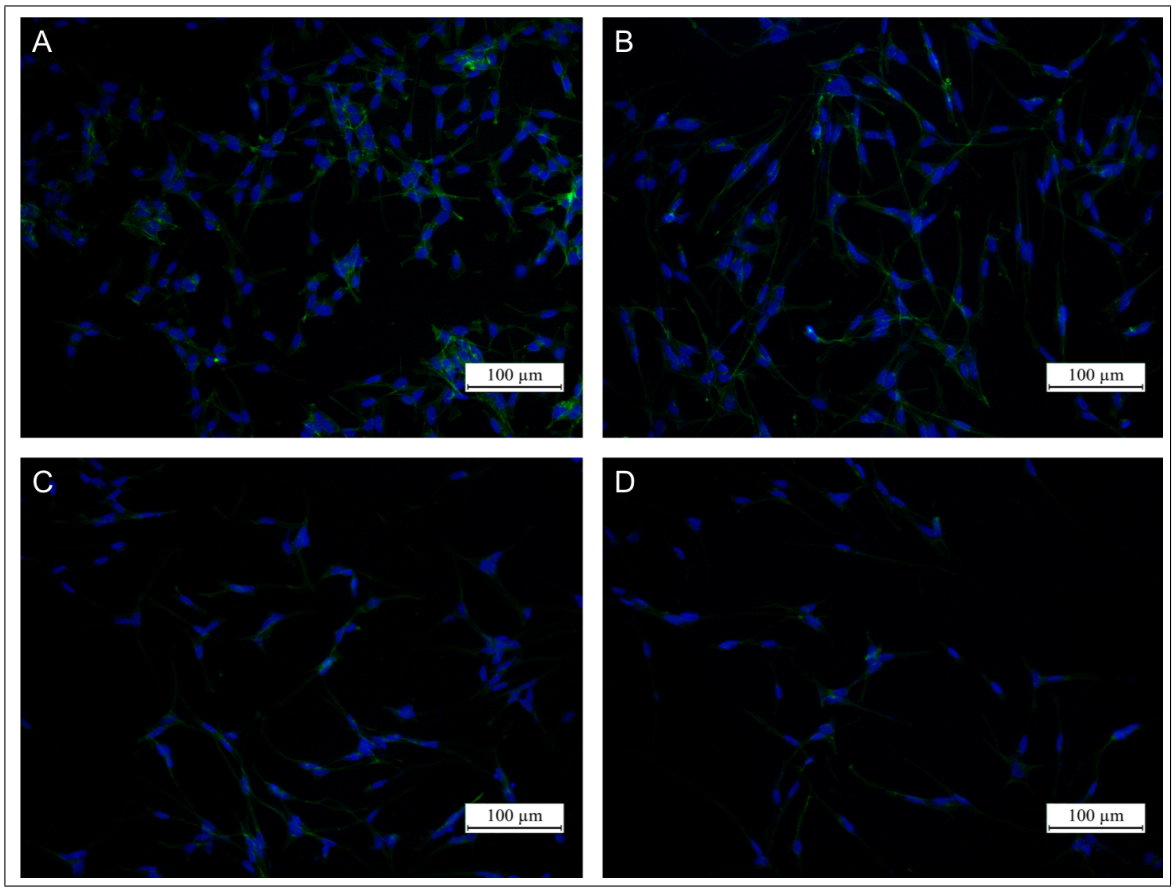

Figure 4.9 20x zoomed images of the F-actin & DAPI stained images of (A) undiff, (B) RA, (C) RB and (D) RBCE groups. Green structures are F-actin filaments, blue structures are DAPI stained nuclei.

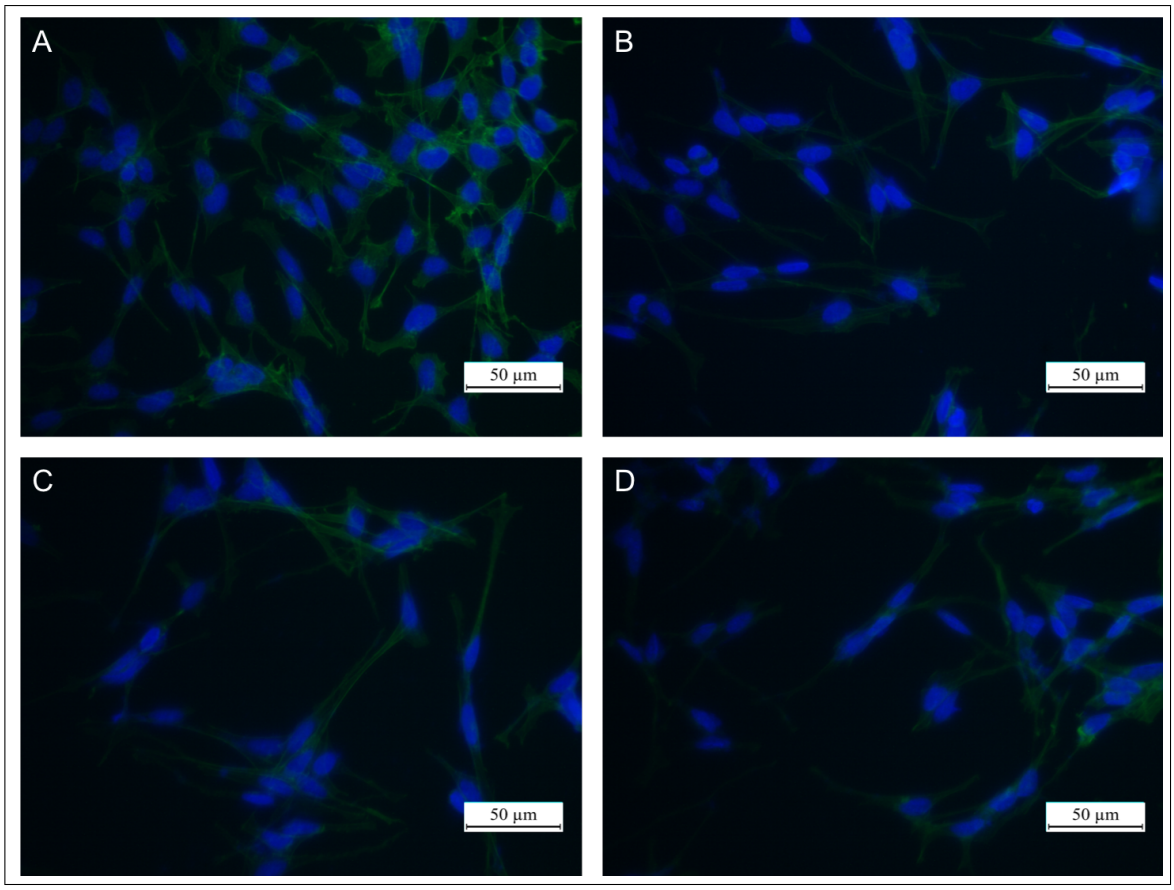

Figure 4.10 40x zoomed images of the F-actin & DAPI stained images of (A) undiff, (B) RA, (C) RB and (D) RBCE groups. Green structures are F-actin filaments, blue structures are DAPI stained nuclei.

Number of cells in ten images collected from each experimental group was counted using ImageJ, and resulting cell numbers are given in Figure 4.11. Only in RBCE treated group, the number of cells statistically significantly decreased compared to control.

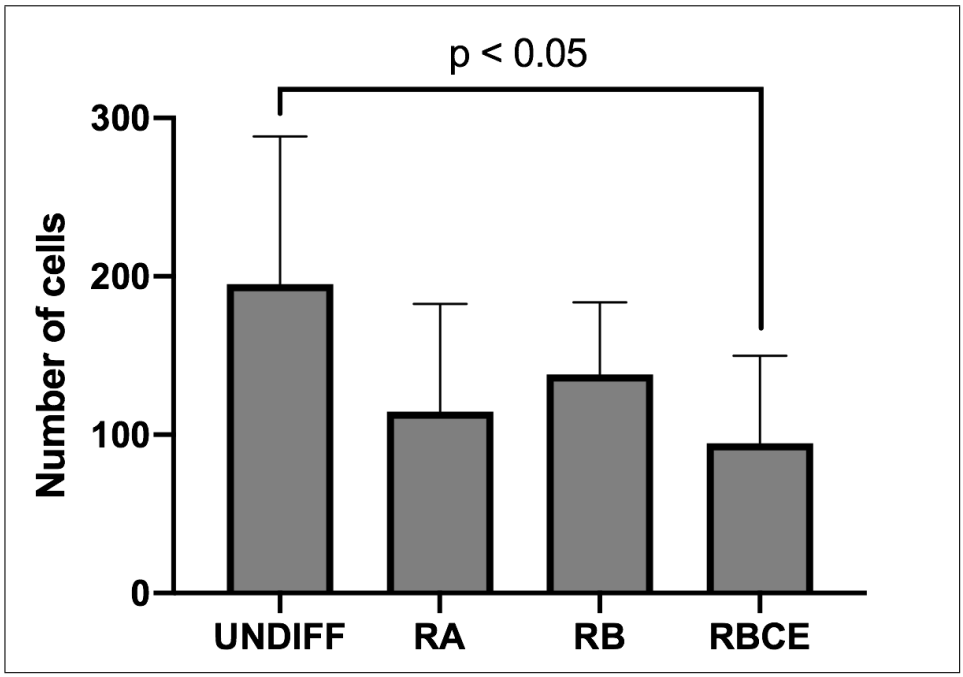

Figure 4.11 Number of cells in each experimental group counted using DAPI stained nuclei.

4.2 Evaluation of the Neuroprotective Effects of Sideritis brevibracteata

4.2.1 Electrophysiology

Electrophysiology experiments were not successful. Rotenone treated cells were unresponsive to negative suctions applied to form gigaseals. This problem resulted in the need for application of the cell viability tests.

4.2.2 Cell Viability Tests

Cell viability tests were performed to find out the toxicity effects of different concentrations of rotenone and then to evaluate the protective effects of *S. brevibracteata*.

4.2.2.1 MTT Assay. MTT assay was performed twice and both yielded very low absorbance values. When it was tried for the third time, the absorbances become slightly higher. Resulting cell viability graph is given in Figure 4.12. According to the graph, increasing rotenone concentrations increased cell viability up to 50 nM.

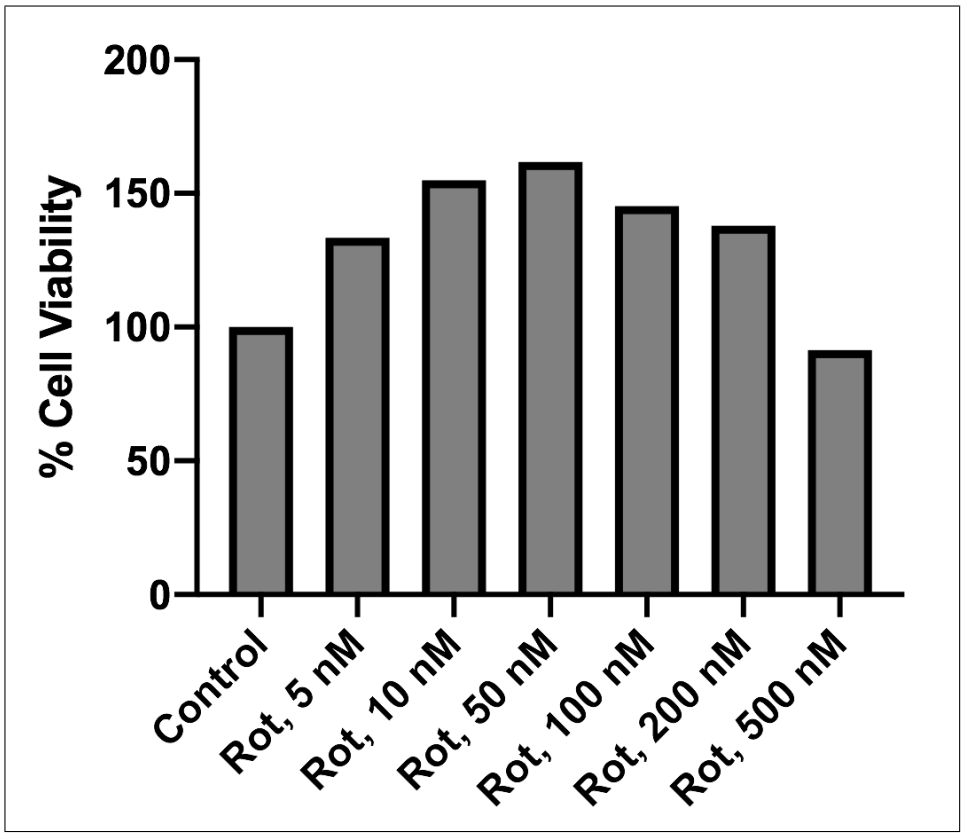

Figure 4.12 MTT cell viability assay with different rotenone concentrations.

4.2.2.2 AO/PI Staining. For AO/PI experiments, higher rotenone concentrations were preferred. Cells in the collected images were counted using ImageJ. Number of dead cells were subtracted from number of all cells, to have the number of live cells. The results of the rotenone toxicity analysis is given in Figure 4.13.

This graph showed three important points; (i) Control groups with and without the vehicle (DMSO) can statistically be considered the same, (ii) for observing toxicity, 24 hour incubation is crucial and (iii) 20 µM rotenone decreases cell viability 50%.

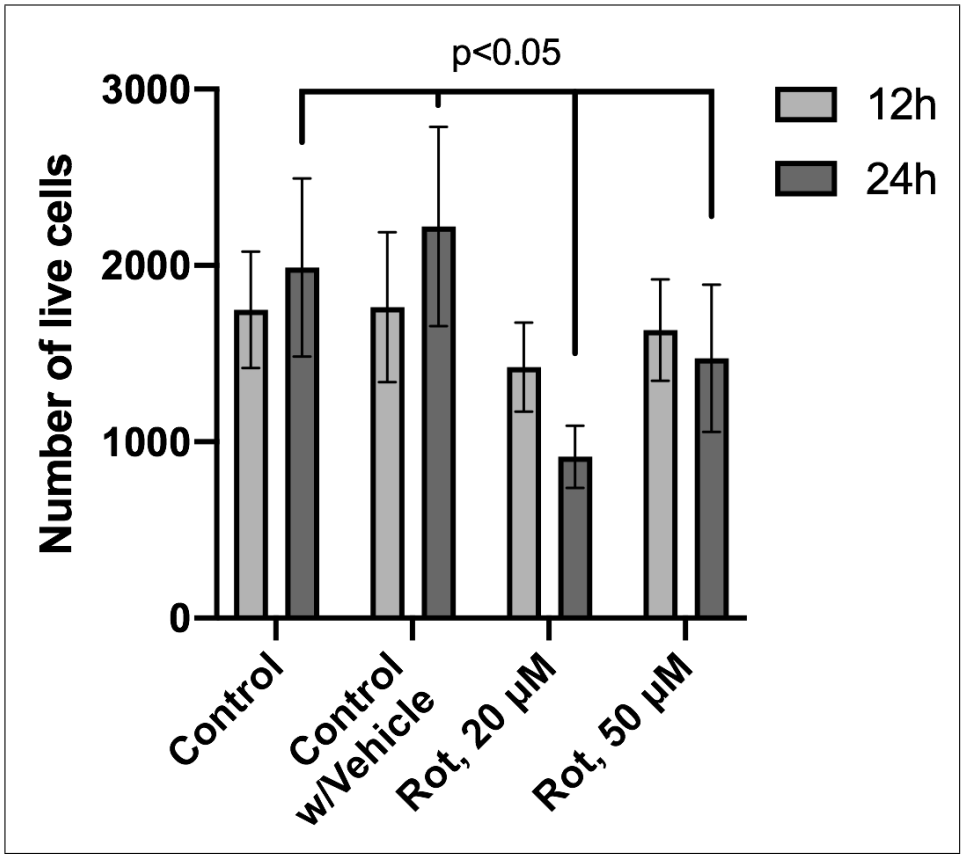

Figure 4.13 Rotenone toxicity analysis.

Taking previous results into consideration, analyses with *S. brevibracteata* was performed. As control group had no difference with control group containing vehicle, only the second group was used. Selected rotenone application was 20 µM for 24 hours. Resulting images are given in Figure 4.14 - 4.21.

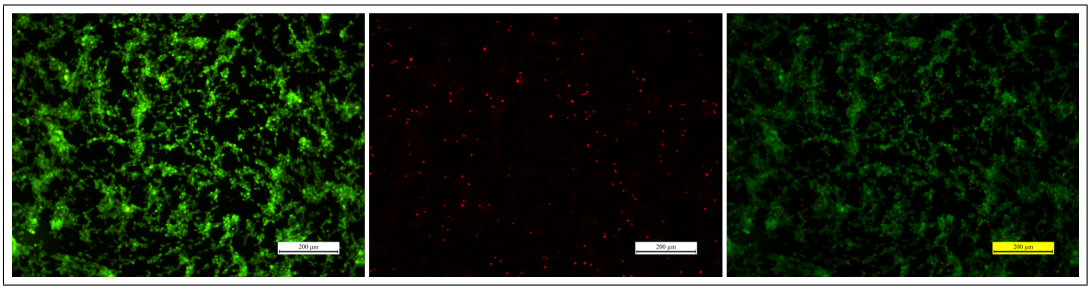

Figure 4.14 Acridine orange/Propidium iodide (AO/PI) images of control cells w/Vehicle collected using fluorescence microscopy. Green cells are stained with AO and they contain both dead and live cells. Red cells are stained with PI and they are dead cells.

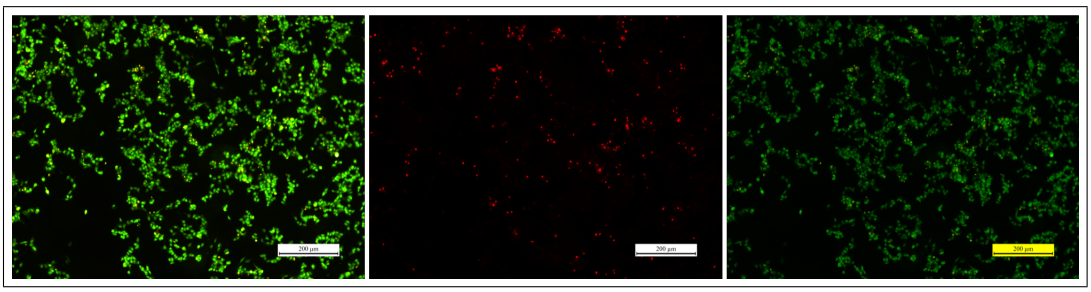

Figure 4.15 AO/PI images of 20 µM Rotenone treated cells.

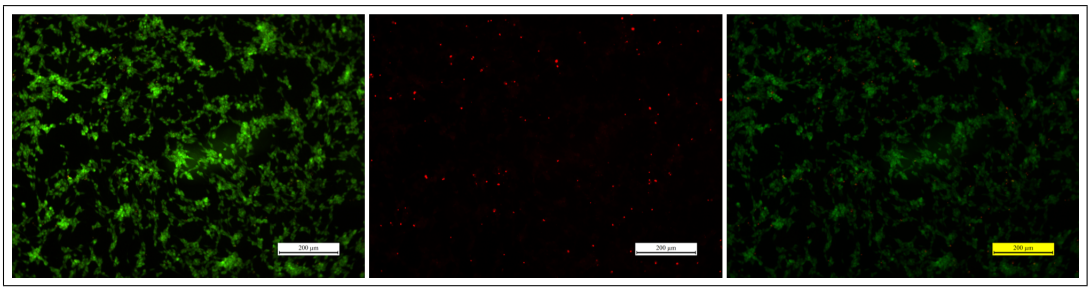

Figure 4.16 AO/PI images of 1 µg/mL *S. brevibracteata* treated cells.

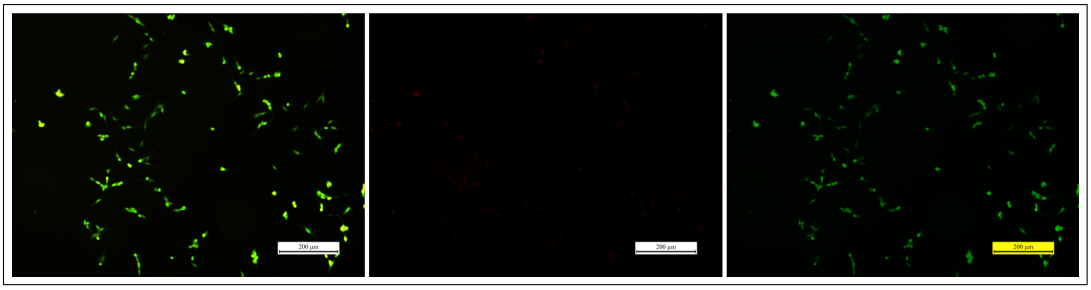

Figure 4.17 AO/PI images of 5 µg/mL *S. brevibracteata* treated cells.

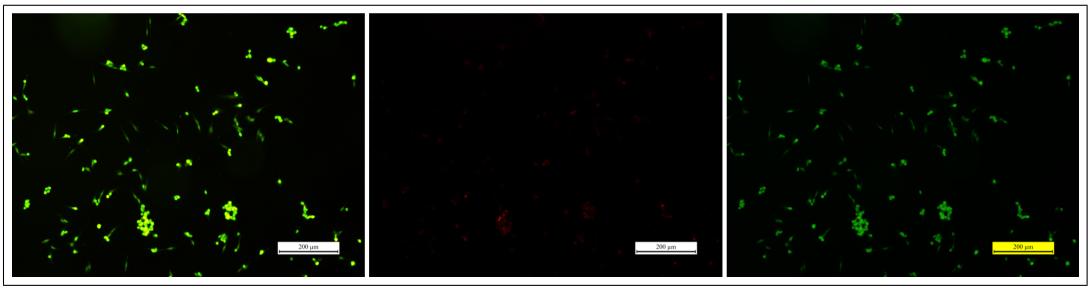

Figure 4.18 AO/PI images of 10 µg/mL *S. brevibracteata* treated cells.

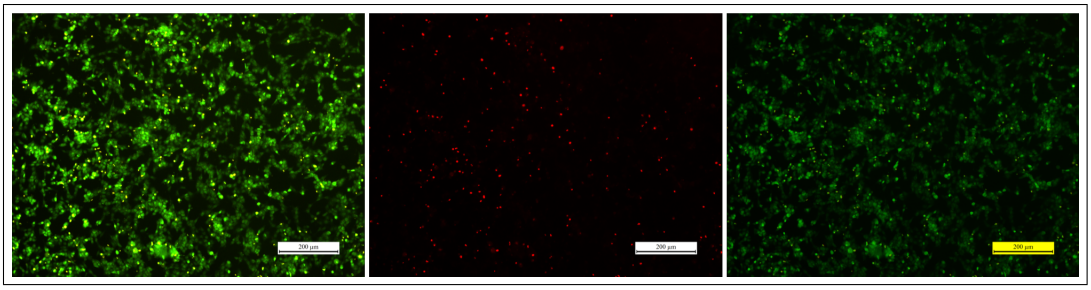

Figure 4.19 AO/PI images of 20 µM Rotenone and 1 µg/mL *S. brevibracteata* treated cells.

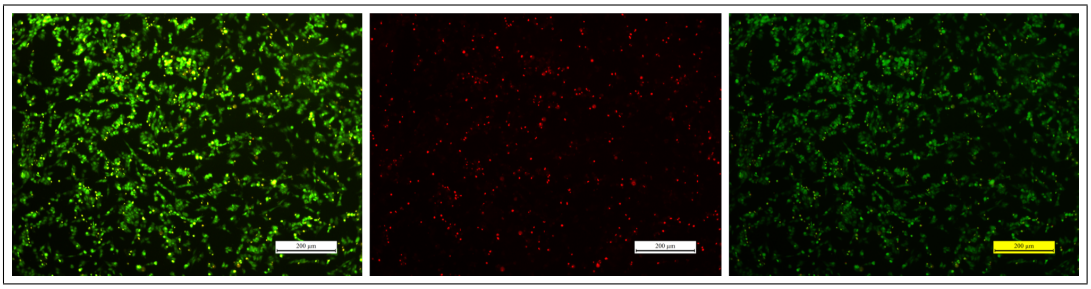

Figure 4.20 AO/PI images of 20 µM Rotenone and 5 µg/mL *S. brevibracteata* treated cells.

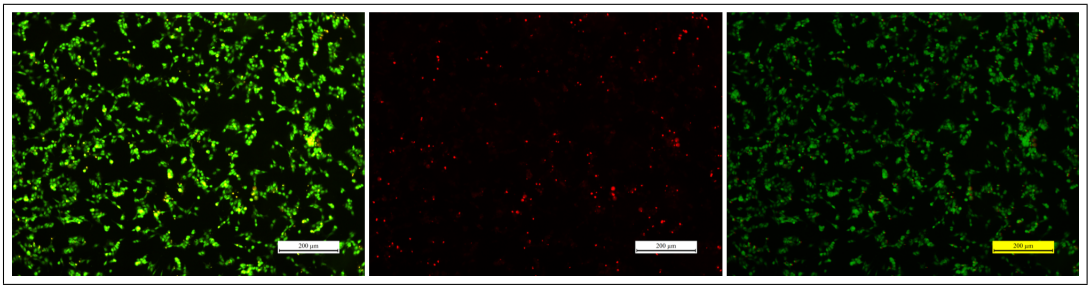

Figure 4.21 AO/PI images of 20 µM Rotenone and 10 µg/mL *S. brevibracteata* treated cells.

The resulting graphs for the evaluation of the toxic effects of *S. brevibracteata* is given in Figure 4.22. It was found that the n-butanol extract of *S. brevibracteata* becomes toxic to cells starting from the 5 µg/mL concentration.

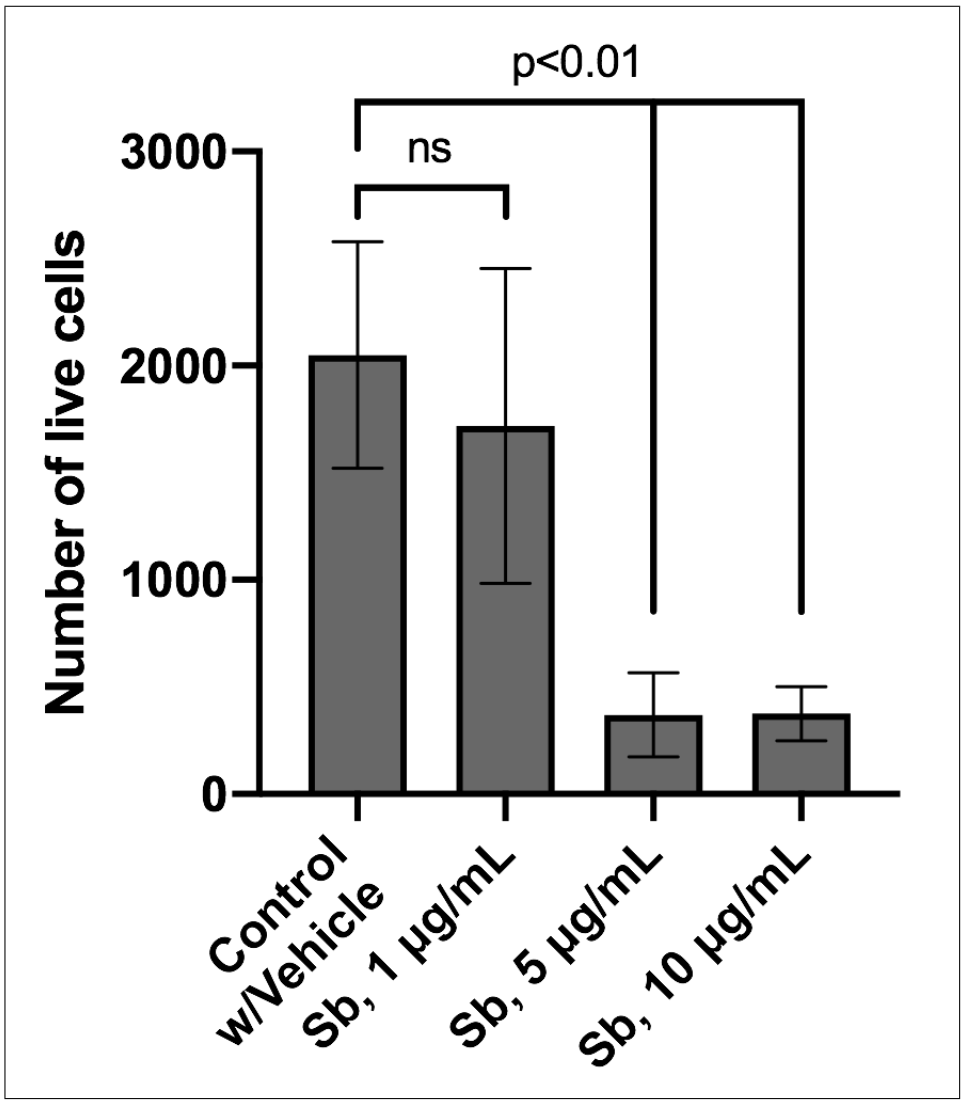

Figure 4.22 *S. brevibracteata* toxicity analysis.

The results of the investigation of the protective effects of *S. brevibracteata* against rotenone induced neurodegeneration is given in Figure 4.23. According to the graph, 1 µg/mL *S. brevibracteata* group is not different than the control group. It is statistically significantly different than the rotenone group.

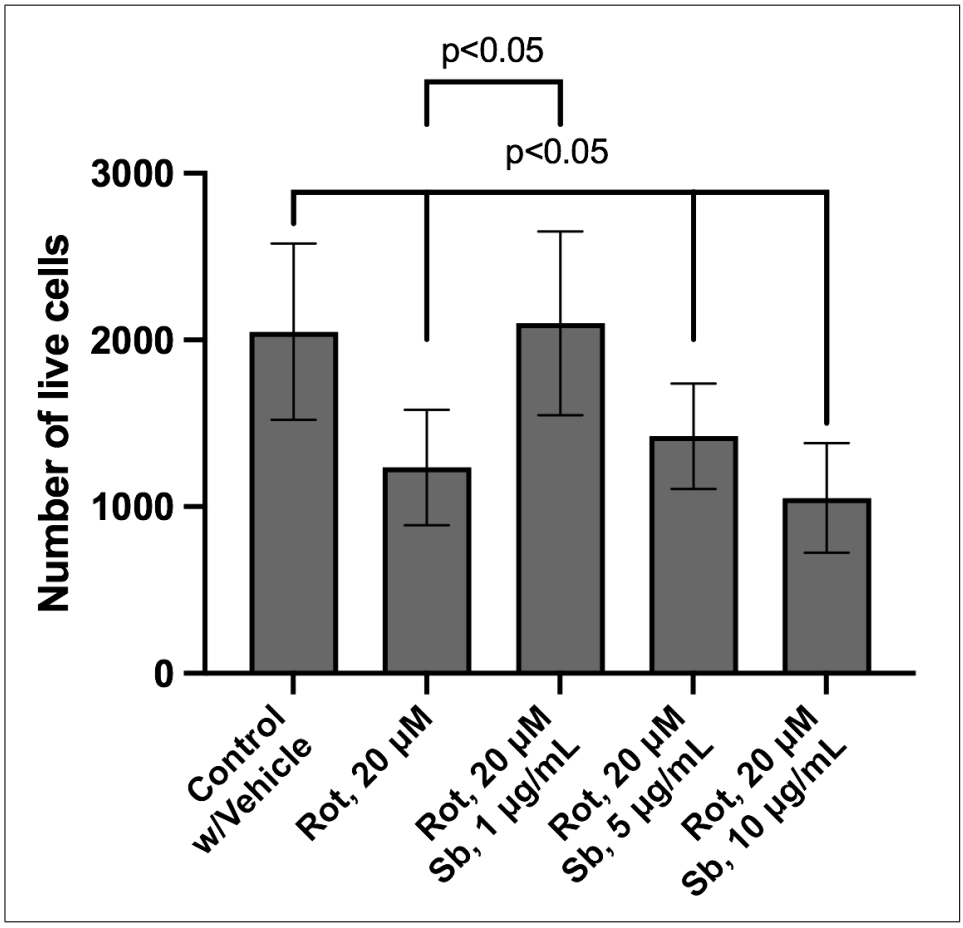

Figure 4.23 Evaluation of the protective effects of *S. brevibracteata* against 20 µM rotenone induced toxicity.

5. DISCUSSION

5.1 Differentiation of Neuroblastoma Cells into Neuron Like Cells

Models for neuroscience research range from using brain slices of different animals to primary neuronal cultures and *in vitro* neuron-like cultures. As neuroscience studies become more and more widely conducted, the pitfalls of these models started to be investigated, more closely. Using brain slices and primary rodent neuronal cultures is an important method, however, differences between human and rodent brains should not be overlooked. Instead of using rodent cells, human stem cells can be differentiated into neurons but understanding and incorporating optimal differentiation methods are necessary to obtain cells that resemble real neurons as much as possible.

SH-SY5Y cell line is widely used as an *in vitro* neuronal model and also as a neuroblastoma cancer model. There are many studies where these cells are considered to be neuron-like cells in their undifferentiated form, in which they are cancer cells, in principle. Goldie et al. looked into the studies using SH-SY5Y cells between the years of 2000 and 2014 and they have shown that among 2307 articles, only 393 of them used a differentiation protocol in their experiments. Among the 393 studies, 283 used RA, 45 of which also included BDNF in their differentiation protocol [65]. Another review reported that among the 962 studies using SH-SY5Y cells as a model of Parkinson's Disease, 159 incorporated a differentiation protocol and only 13 of them used both RA and BDNF [66].

At the time of writing this thesis, a PubMed search of the keywords patch-clamp and SH-SY5Y resulted in 96 articles for human species. When the search is updated to include the word "differentiated", the number of results decreases to 21. If the differentiating agents retinoic acid and brain-derived neurotrophic factor are also added to the search, only 1 article can be found in the PubMed database [20], where

the researchers investigated the inwardly rectifying human ether-a-go-go related gene (HERG) coded inward K^+ currents.

The absence of a commonly agreed differentiation protocol might be the reason for the small number of studies that include a differentiation protocol. Also, the required laboratory work and expense of differentiation protocols might be the other reasons for the preference of undifferentiated neuroblastoma cells for research. But our results clearly show that undifferentiated cells cannot be accepted as a neuron model.

RA induced differentiation withdraws cells from the cell cycle and stops cell proliferation. It increases the expression of membrane-associated cytoskeletal elements and other neuron-specific proteins [5]. Even though BDNF is a growth promoting agent and it induces proliferation, application of RA prior to BDNF helps keep cells in their non-proliferating state and BDNF acts for further neuronal differentiation. Also, BDNF was found to increase the sodium channel expression in PC12 cells [67].

In patch-clamp experiments, we observed that successful patching of the cells, when they were treated with a high concentration of RA (10 µM), was difficult because of the increased rigidity of the membrane. This high rigidity might be due to the overexpression of membrane-associated cytoskeletal proteins such as doublecortin, vimentin, neurofilament-68 and tau [18]. In our experiments, the differentiation of SH-SY5Y human neuroblastoma cells was done by using 1 µM RA application to the medium. In our hands, low concentration of RA (1 µM) has provided more successful recordings from these cells.

According to our results, patch-clamp experiments performed on SH-SY5Y neuroblastoma cells showed that undifferentiated cells exhibited little or no inward currents. On the other hand, the outward currents, which are the potassium currents had high amplitudes (150-300 pA). The undifferentiated cells had the highest amplitude of outward currents among the other experimental groups. This finding is not surprising in the sense that K^+ channels are generally more active in cancer cells than normal cells. Dysregulation of potassium channels is implicated in several important aspects

of cancer initiation and progression. The K^+ channel subgroup responsible for the high amplitude of outward currents in undifferentiated neuroblastoma cells has been identified to be big Ca^{2+} activated potassium channels (BK) with minor contributions from small Ca^{2+} activated potassium channels (SK) and other Kv channels [68]. However, another study concludes that these currents are due to the delayed rectifier potassium channels with no significant effect from A-type or calcium-dependent potassium channels [19].

Even though RA differentiated cells show statistically significantly lower potassium currents compared to UNDIFF cells, their inward currents are still lower compared to RA + BDNF treated cells. However, higher sample sizes are required to draw certain conclusions.

Inward currents, which are the sodium currents of the RB group have the highest amplitude among inward currents of all experimental groups. Previously, it was observed that BDNF increases the expression of sodium channels in PC12 cells via its actions on TrkB receptors [67]. Our results were consistent with this finding.

The high amplitude of K^+ currents and the absence of Na^+ currents in undifferentiated cells with the low amplitudes of Na^+ currents in RA differentiated cells, support the necessity of the application of RA + BDNF as differentiating agents in SH-SY5Y cells. Electrophysiological measurements are one of the most accurate methods that can prove successful differentiation.

Western blot analyses showed different trends for the proteins of interest. Previous studies investigating the expression of TUJ1 and SYN in SH-SY5Y cells showed that the expression of these proteins increased with differentiation, however, they failed to report statistically significant results [7, 69]. In our experiments, we found that TUJ1 expression statistically significantly increased only in experimental groups including BDNF (RB & RBCE, $p < 0.05$). As a neuron-specific protein, TUJ1 expression is considered to be one of the important markers of neurons. Even though it is found in undifferentiated neuroblastoma cells as well, it is expected to increase with differenti-

ation in neurons [8, 69]. The statistically significant increase of TUJ1 in the presence of BDNF shows that presence of BDNF is essential for the differentiation of SH-SY5Y cells to neurons.

SYN protein is involved in several different processes in neurons, including synaptic biogenesis, vesicle protein sorting and exocytosis and endocytosis [70]. However, it can be used as a clinical marker for neuroblastoma tumors and more generally for neuroendocrine tumors [71]. Western blot results of our experiments show a statistically significant decrease of SYN protein upon differentiation of neuroblastoma cells into neurons ($p < 0.05$), which is consistent with the clinical usage of this protein as a tumor marker. However, we also observed an increase in RBCE group compared to the RA group ($p < 0.05$). This is thought to be due to the upregulation of SYN expression in the presence of CHOL and E2 [72, 73].

F-Actin & DAPI stainings showed that the F-actin filaments are gathered closer to the nuclei in undifferentiated cells compared to other groups. However, especially in the RB group, the F-actin bands are more structurally organized and they are elongated through the neurites. This may be due to the increased expression of neuron-specific cytoskeletal proteins such as TUJ1.

When the number of DAPI stained nuclei was counted, it was found that in RBCE group, the number of cells statistically significantly decreased with respect to undifferentiated cells. This is in line with our observations that the vehicles (ethanol and DMSO) used to dissolve CHOL and E2 exceeds the limits of safe application of these vehicles on the cells.

To summarize, several interesting and remarkable points can be deduced from the electrophysiology recordings, Western blot and immunocytochemistry analyses performed. Undifferentiated SH-SY5Y human neuroblastoma cells are cancer cells and differentiation of these cells are essential for their consideration as a model in neurodegenerative disease studies. High amplitude outward (potassium) and low amplitude inward (sodium) currents observed in undifferentiated cells are not a characteristic

property of the neurons. Also, the high expression of SYN in undifferentiated cells strongly indicate the cancerous biochemical structure of the SH-SY5Y cells.

RA treatment alone cannot fully differentiate neuroblastomas into neuron-like cells. Our electrophysiological recordings showed a decrease in outward currents of the RA group, however inward current amplitudes were still small compared to RB and RBCE groups. In addition, TUJ1 expression did not statistically significantly increased in RA group, whereas both RB and RBCE groups showed higher TUJ1 expressions ($p < 0.05$) as an indicator of increased β-tubulin expression in differentiated SH-SY5Y cells. This implies the need for BDNF to accompany RA for a complete differentiation.

Lastly, the addition of CHOL and E2 to the medium does not provide any additional benefits for the differentiation. The electrophysiological and biochemical comparisons of RB and RBCE did not show statistically significant differences. In light of our experiments, we conclude that undifferentiated SH-SY5Y human neuroblastoma cells cannot be used to model neurons, but differentiation allows these cells to be considered neurons. And, to induce differentiation of SH-SY5Y human neuroblastoma cells into neurons RA and BDNF application is required, however, CHOL and E2 are not essential.

5.2 Evaluation of the Neuroprotective Effects of Sideritis brevibracteata

S. brevibracteata showed a statistically significant effect in terms of neuroprotection when it is applied at a concentration of 1 µg/mL. However at higher doses, it is toxic to the cells. Further investigations are required including increasing the sample sizes and repeating the experiments with different flavonoids that are purified from the *S. brevibracteata* extract. Also, changing the drug treatment times are necessary in order to evaluate the time dependency of this protection.

The effective concentration of 1 µg/mL was significant in the sense that in a previous study, the purified flavonoids from *S. brevibracteata* showed antioxidant IC50 values ranging from 0.57 to 3.48 µg/mL [58]. However, in a study that investigates the *S. brevibracteata* extract as a whole, it was found that the extract had 160 µg/mL antioxidant IC50 [57]. The discrepancy in the effective concentrations may be explained with the fact that in the referred study, liposomes was used to evaluate the antioxidant effect of the extract.

Electrophysiological recordings could not be collected from rotenone treated cells. This may be due to the increased stiffness of the rotenone treated cells which resulted in the inability of cells to approach the patch pipette. MTT tests were also not successful. The observed effect of concentration dependant toxicity of rotenone could not be observed using MTT. Higher number of cell per well values may be necessary in order to collect data from the MTT readings of these type of cells. Also, lower concentrations of rotenone used in MTT analyses may also have caused the meaningless results.

6. CONCLUSION

Some biological questions can be most accurately answered when an interdisciplinary approach is employed. The combination of the results from patch-clamp, Western blot and immunocytochemistry investigations presented here gives a broad perspective when trying to answer the question of the optimal differentiation of SH-SY5Y human neuroblastoma cells. After thorough experimentation and analyses, we conclude that undifferentiated SH-SY5Y cells should not be used as a model for neurons, and it is necessary and sufficient to use 1 µM RA and 10 ng/mL BDNF to induce neuronal differentiation of these cells. CHOL and E2 have minimal additional effects in promoting neuronal differentiation, hence their application is not a requirement.

The second part of this thesis yielded in an exciting finding, which is the observed protective effect of *S. brevibracteata* against rotenone induced neurotoxicity modeled in differentiated SH-SY5Y human neuroblastoma cells. Further investigations are required to understand whether and how *S. brevibracteata* can be employed in helping patients with Parkinson's Disease.

APPENDIX A.
Identification of Inward and Outward Currents

This part of the study was conducted by both myself and Gül Öncü.

The characteristics of inward and outward currents in the electrophysiological recordings were investigated by blocking sodium and potassium channels. To isolate inward currents, KCl in the intracellular pipette solution was replaced with the same concentration of cesium chloride (CsCl) to block the Kv channels [74, 75]. Doing so, we found that outward currents almost entirely diminished in the presence of CsCl. Being CsCl sensitive, these currents were shown to be the K^+ currents. This finding is not surprising in the sense that K^+ channels are generally more active in cancer cells than normal cells. Dysregulation of potassium channels is implicated in several important aspects of cancer initiation and progression.

To make sure that the inward currents were also eliminated, NaCl was replaced by the same concentration of $NMDG^+$. When Na^+ ions in the extracellular solution were replaced with $NMDG^+$, the inward current was abolished, indicating that Na^+ ions were responsible for this current.

APPENDIX B.

Atomic Force Microscopy

This part of the study was conducted by myself, Gül Öncü and Lt. Commander Dr. Doğuş Özkan from Turkish Naval Academy

Atomic Force Microscopy (AFM) is a powerful device for obtaining three-dimensional high resolution topographical images, and real-time, quantitative elasticity characteristics of living cells. AFM measurements in this study were taken using probes with silicon nitride tips and spring constants of 0.178 N/m. Averages of 10 Young's modulus measurements from 4 different cells from each group were taken into consideration for comparison of the nanomechanical characteristics of the undifferentiated and RA and BDNF treated (RB) SH-SY5Y human neuroblastoma cells. Measurements were taken at day 8 of differentiation. To ensure cell viability, all experiments have been completed in under 2 hours after cells were taken from the incubator.

Figure B.1.a shows the AFM image of an undifferentiated SH-SY5Y human neuroblastoma cell and one force curve result which was extracted from the area labeled with red rectangle. Average Young's modulus of the undifferentiated SH-SY5Y cells was found to be 3618.44 Pa $\pm$ 1153.98, while the average Young's modulus of the RA and BDNF treated SH-SY5Y cells was 6884.31 Pa $\pm$ 3725.29 (see Figure B.1.b). The increase in stiffness upon differentiation was found to be not statistically significantly different according to ANOVA. This may be due to the low number of samples (n=4). However, the softer undifferentiated cells were observed to be very sticky and harder to separate from the AFM probe. The number of samples should be increased to be able to draw certain conclusions.

Information about the stiffness of the cells is accepted as a good indicator of the physiological state of the cells [76]. Although tumors are sensed to be stiff masses; single cancer cells are found to be softer than their normal counterparts [77]. Being

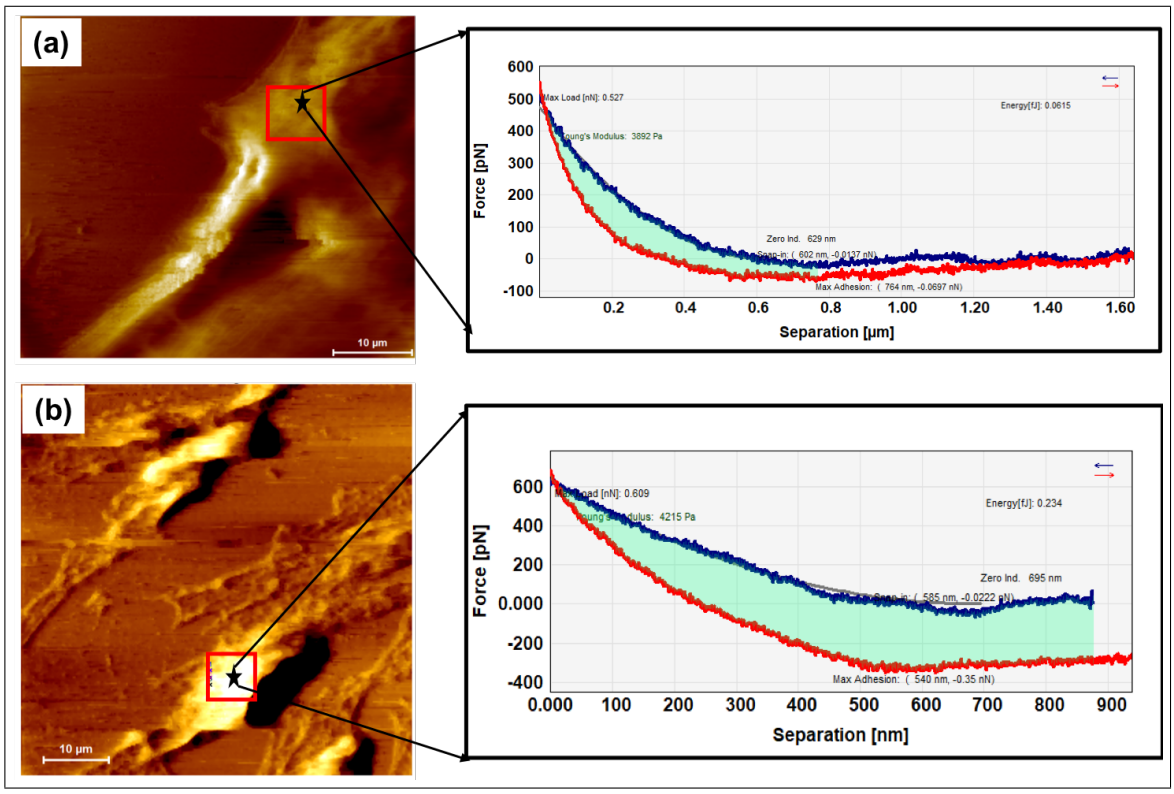

Figure B.1 Topography images and force-distance curves collected from a) UNDIFF, b) RB treated cells.

more deformable, cancer cells can move, migrate and divide more easily. Young's modulus data collected from UNDIFF and RB groups in our study are in accordance with this information. RB cells were found to be almost two times stiffer than the UNDIFF cells.

Elastic properties of the cells are correlated with the amount of actin that they carry. The softness of single cancer cells is attributed to the loss and disorganization of actin filaments and microtubules [77]. Having very long extensions throughout the organism, neurons rely on the structural integrity and the stability stemming from the increased amount of membrane-associated cytoskeletal elements. This is evident in our AFM and Western blot analyses where the stiffness of the cells and the expression of β-tubulin increase. Also, in F-actin & DAPI staining, actin filaments were observed to be more organized in RB group, compared to the undifferentiated cells.

REFERENCES

1. Ke, Z., X. Zhang, Z. Cao, Y. Ding, N. Li, L. Cao, T. Wang, C. Zhang, G. Ding, Z. Wang, X. Xu, and W. Xiao, "Drug discovery of neurodegenerative disease through network pharmacology approach in herbs," *Biomedicine & Pharmacotherapy*, Vol. 78, pp. 272–279, Mar. 2016.

2. Baig, M. H., K. Ahmad, M. Saeed, A. M. Alharbi, G. E. Barreto, G. M. Ashraf, and I. Choi, "Peptide based therapeutics and their use for the treatment of neurodegenerative and other diseases," *Biomedicine & Pharmacotherapy*, Vol. 103, pp. 574–581, July 2018.

3. Biedler, J. L., L. Helson, and B. A. Spengler, "Morphology and Growth, Tumorigenicity, and Cytogenetics of Human Neuroblastoma Cells in Continuous Culture," *Cancer Research*, Vol. 33, pp. 2643–2652, 1973.

4. Kovalevich, J., and D. Langford, "Considerations for the Use of SH-SY5Y Neuroblastoma Cells in Neurobiology," in *Neuronal Cell Culture* (Amini, S., and M. K. White, eds.), Vol. 1078, pp. 9–21, Totowa, NJ: Humana Press, 2013.

5. Shipley, M. M., C. A. Mangold, and M. L. Szpara, "Differentiation of the SH-SY5Y Human Neuroblastoma Cell Line," *Journal of Visualized Experiments*, no. 108, pp. 1–11, 2016.

6. Agholme, L., T. Lindström, K. Kågedal, J. Marcusson, and M. Hallbeck, "An In Vitro Model for Neuroscience: Differentiation of SH-SY5Y Cells into Cells with Morphological and Biochemical Characteristics of Mature Neurons," *Journal of Alzheimer's Disease*, Vol. 20, pp. 1069–1082, June 2010.

7. Constantinescu, R., A. T. Constantinescu, H. Reichmann, and B. Janetzky, "Neuronal differentiation and long-term culture of the human neuroblastoma line SH-SY5Y," in *Neuropsychiatric Disorders An Integrative Approach* (Gerlach, M., J. Deckert, K. Double, and E. Koutsilieri, eds.), Vol. 72, pp. 17–28, Vienna: Springer Vienna, 2007.

8. Krishtal, J., O. Bragina, K. Metsla, P. Palumaa, and V. Tõugu, "In situ fibrillizing amyloid-beta 1-42 induces neurite degeneration and apoptosis of differentiated SH-SY5Y cells," *PLOS ONE*, Vol. 12, pp. 1–16, Oct. 2017.

9. Påhlman, S., A.-I. Ruusala, L. Abrahamsson, M. E. Mattsson, and T. Esscher, "Retinoic acid-induced differentiation of cultured human neuroblastoma cells: A comparison with phorbolester-induced differentiation," *Cell Differentiation*, Vol. 14, pp. 135–144, June 1984.

10. Encinas, M., M. Iglesias, Y. Liu, H. Wang, A. Muhaisen, V. Ceña, C. Gallego, and J. X. Comella, "Sequential Treatment of SH-SY5Y Cells with Retinoic Acid and Brain-Derived Neurotrophic Factor Gives Rise to Fully Differentiated, Neurotrophic Factor-Dependent, Human Neuron-Like Cells," *Journal of Neurochemistry*, Vol. 75, pp. 991–1003, Jan. 2002.

11. Teppola, H., J.-R. Sarkanen, T. O. Jalonen, and M.-L. Linne, "Morphological Differentiation Towards Neuronal Phenotype of SH-SY5Y Neuroblastoma Cells by Estradiol, Retinoic Acid and Cholesterol," *Neurochemical Research*, Vol. 41, pp. 731–747, Apr. 2016.

12. Edsjö, A., E. Lavenius, H. Nilsson, J. C. Hoehner, P. Simonsson, L. A. Culp, T. Martinsson, C. Larsson, and S. Påhlman, "Expression of trkB in Human Neuroblastoma in Relation to MYCN Expression and Retinoic Acid Treatment," *Laboratory Investigation*, Vol. 83, pp. 813–823, June 2003.

13. Cernaianu, G., P. Brandmaier, G. Scholz, O. P. Ackermann, R. Alt, K. Rothe, M. Cross, H. Witzigmann, and R. B. Tröbs, "All-trans retinoic acid arrests neuroblastoma cells in a dormant state. Subsequent nerve growth factor/brain-derived neurotrophic factor treatment adds modest benefit," *Journal of Pediatric Surgery*, Vol. 43, pp. 1284–1294, July 2008.

14. Janardhanan, A., A. Sadanand, and A. J. Vanisree, "Synapsin III in Differentiated Shsy5y Cell Line as a Potential Tool for Neuropharmacological Evaluations in Schizophrenia," *Electronic Journal of Biology*, p. 9, 2018.

15. Matsumoto, K., R. K. Wada, J. M. Yamashiro, D. R. Kaplan, and C. J. Thiele, "Expression of Brain-derived Neurotrophic Factor and p!45TrkB Affects Survival, Differentiation, and Invasiveness of Human Neuroblastoma Cells," *Cancer Research*, Vol. 55, pp. 1798–1806, 1995.

16. Zhao, S., A. Stamm, J. S. Lee, A. Gruverman, J. Y. Lim, and L. Gu, "Elasticity of Differentiated and Undifferentiated Human Neuroblastoma Cells Characterized by Atomic Force Microscopy," *Journal of Mechanics in Medicine and Biology*, Vol. 15, pp. 1–10, Oct. 2015.

17. Nishida, Y., N. Adati, R. Ozawa, A. Maeda, Y. Sakaki, and T. Takeda, "Identification and classification of genes regulated by phosphatidylinositol 3-kinase- and TRKB-mediated signalling pathways during neuronal differentiation in two subtypes of the human neuroblastoma cell line SH-SY5Y," *BMC Research Notes*, Vol. 1, no. 95, pp. 1–11, 2008.

18. Halitzchi, F., L. Jianu, and B. Amuzescu, "Electrophysiology and Pharmacology Study of a Human Neuroblastoma Cell Line," *Romanian Reports in Physics*, Vol. 67, no. 2, pp. 439–451, 2015.

19. Tosetti, P., V. Taglietti, and M. Toselli, "Functional Changes in Potassium Conductances of the Human Neuroblastoma Cell Line SH-SY5Y During In Vitro Differentiation," *Journal of Neurophysiology*, Vol. 79, pp. 648–658, Feb. 1998.

20. Arcangeli, A., B. Rosati, O. Crociani, A. Cherubini, L. Fontana, B. Passani, E. Wanke, and M. Olivotto, "Modulation of HERG current and herg gene expression during retinoic acid treatment of human neuroblastoma cells: Potentiating effects of BDNF," *Journal of Neurobiology*, Vol. 40, pp. 214–225, Aug. 1999.

21. Towbin, H., T. Staehelin, and J. Gordon, "Electrophoretic transfer of proteins from polyacrylamide gels to nitrocellulose sheets: Procedure and some applications.," *Proceedings of the National Academy of Sciences*, Vol. 76, pp. 4350–4354, Sept. 1979.

22. Burnette, W., ""Western Blotting": Electrophoretic transfer of proteins from sodium dodecyl sulfate-polyacrylamide gels to unmodified nitrocellulose and radiographic detection with antibody and radioiodinated protein A," *Analytical Biochemistry*, Vol. 112, pp. 195–203, Apr. 1981.

23. Wulf, E., A. Deboben, F. A. Bautz, H. Faulstich, and T. Wieland, "Fluorescent phallotoxin, a tool for the visualization of cellular actin.," *Proceedings of the National Academy of Sciences*, Vol. 76, pp. 4498–4502, Sept. 1979.

24. Tarnowski, B. I., F. G. Spinale, and J. H. Nicholson, "DAPI as a Useful Stain for Nuclear Quantitation," *Biotechnic & Histochemistry*, Vol. 66, pp. 296–302, Jan. 1991.

25. Sontheimer, H., *Diseases of the Nervous System*, Amsterdam ; Boston: Elsevier/AP, Academic Press is an imprint of Elsevier, 2015. OCLC: ocn918994176.

26. Raza, C., R. Anjum, and N. u. A. Shakeel, "Parkinson's disease: Mechanisms, translational models and management strategies," *Life Sciences*, Vol. 226, pp. 77–90, June 2019.

27. Leisman, G., R. Melillo, and F. R., "Clinical Motor and Cognitive Neurobehavioral Relationships in the Basal Ganglia," in *Basal Ganglia - An Integrative View* (Barrios, F. A., ed.), InTech, Jan. 2013.

28. Hely, M. A., V. S. Fung, and J. G. Morris, "Treatment of Parkinson's disease," *Journal of Clinical Neuroscience*, pp. 484–494, 2000.

29. Staff, R., "Pfizer ends research for new Alzheimer's, Parkinson's drugs," *Reuters*, July 2018.

30. Sezgin, Z., and Y. Dincer, "Alzheimer's disease and epigenetic diet," *Neurochemistry International*, Vol. 78, pp. 105–116, Dec. 2014.

31. Sohn, E., "A quest to stave off the inevitable," *Nature*, Vol. 559, pp. 18–120, July 2018.

32. Valls-Pedret, C., A. Sala-Vila, M. Serra-Mir, D. Corella, R. de la Torre, M. Á. Martínez-González, E. H. Martínez-Lapiscina, M. Fitó, A. Pérez-Heras, J. Salas-Salvadó, R. Estruch, and E. Ros, "Mediterranean Diet and Age-Related Cognitive Decline: A Randomized Clinical Trial," *JAMA Internal Medicine*, Vol. 175, pp. 1094–1103, July 2015.

33. Mosconi, L., M. Walters, J. Sterling, C. Quinn, P. McHugh, R. E. Andrews, D. C. Matthews, C. Ganzer, R. S. Osorio, R. S. Isaacson, M. J. De Leon, and A. Convit, "Lifestyle and vascular risk effects on MRI-based biomarkers of Alzheimer's disease: A cross-sectional study of middle-aged adults from the broader New York City area," *BMJ Open*, Vol. 8, pp. 1–10, Mar. 2018.

34. Gao, X., H. Chen, T. T. Fung, G. Logroscino, M. A. Schwarzschild, F. B. Hu, and A. Ascherio, "Prospective study of dietary pattern and risk of Parkinson disease," *The American Journal of Clinical Nutrition*, Vol. 86, pp. 1486–1494, Nov. 2007.

35. Livingston, G., A. Sommerlad, V. Orgeta, S. G. Costafreda, J. Huntley, D. Ames, C. Ballard, S. Banerjee, A. Burns, J. Cohen-Mansfield, C. Cooper, N. Fox, L. N. Gitlin, R. Howard, H. C. Kales, E. B. Larson, K. Ritchie, K. Rockwood, E. L. Sampson, Q. Samus, L. S. Schneider, G. Selbæk, L. Teri, and N. Mukadam, "Dementia prevention, intervention, and care," *The Lancet*, Vol. 390, pp. 2673–2734, Dec. 2017.

36. Bernstein, N., M. Akram, M. Daniyal, H. Koltai, M. Fridlender, and J. Gorelick, "Antiinflammatory Potential of Medicinal Plants: A Source for Therapeutic Secondary Metabolites," in *Advances in Agronomy*, Vol. 150, pp. 131–183, Elsevier, 2018.

37. Bektas, A., S. H. Schurman, R. Sen, and L. Ferrucci, "Aging, inflammation and the environment," *Experimental Gerontology*, Vol. 105, pp. 10–18, May 2018.

38. Moore, A. H., M. J. Bigbee, G. E. Boynton, C. M. Wakeham, H. M. Rosenheim, C. J. Staral, J. L. Morrissey, and A. K. Hund, "Non-Steroidal Anti-Inflammatory Drugs in Alzheimer's Disease and Parkinson's Disease: Reconsidering the Role of Neuroinflammation," *Pharmaceuticals*, Vol. 3, pp. 1812–1841, June 2010.

39. Gilgun-Sherki, Y., E. Melamed, and D. Offen, "Anti-Inflammatory Drugs in the Treatment of Neurodegenerative Diseases: Current State," *Current Pharmaceutical Design*, Vol. 12, pp. 3509–3519, 2006.

40. Kim, W.-G., R. P. Mohney, B. Wilson, G.-H. Jeohn, B. Liu, and J.-S. Hong, "Regional Difference in Susceptibility to Lipopolysaccharide-Induced Neurotoxicity in the Rat Brain: Role of Microglia," *The Journal of Neuroscience*, Vol. 20, pp. 6309–6316, Aug. 2000.

41. Finkel, T., and N. J. Holbrook, "Oxidants, oxidative stress and the biology of ageing," *Nature*, Vol. 408, pp. 239–247, Nov. 2000.

42. Nimse, S. B., and D. Pal, "Free radicals, natural antioxidants, and their reaction mechanisms," *RSC Advances*, Vol. 5, no. 35, pp. 27986–28006, 2015.

43. Pham-Huy, L. A., H. He, and C. Pham-Huy, "Free Radicals, Antioxidants in Disease and Health," *Free Radicals and Antioxidants*, Vol. 4, no. 2, p. 8, 2008.

44. Albarracin, S. L., B. Stab, Z. Casas, J. J. Sutachan, I. Samudio, J. Gonzalez, L. Gonzalo, F. Capani, L. Morales, and G. E. Barreto, "Effects of natural antioxidants in neurodegenerative disease," *Nutritional Neuroscience*, Vol. 15, pp. 1–9, Jan. 2012.

45. Özben, T., *Free Radicals, Oxidative Stress, and Antioxidants: Pathological and Physiological Significance*, Boston, MA: Springer, 1998. OCLC: 864225758.

46. Hare, D., S. Ayton, A. Bush, and P. Lei, "A delicate balance: Iron metabolism and diseases of the brain," *Frontiers in Aging Neuroscience*, Vol. 5, 2013.

47. Halliwell, B., and J. M. C. Gutteridge, *Free Radicals in Biology and Medicine*, Oxford, United Kingdom: Oxford University Press, fifth edition ed., 2015.

48. Kim, G. H., J. E. Kim, S. J. Rhie, and S. Yoon, "The Role of Oxidative Stress in Neurodegenerative Diseases," *Experimental Neurobiology*, Vol. 24, no. 4, p. 325, 2015.

49. Adiga, U., and S. Adiga, "Total Antioxidant Activity in Old Age," *Biomedical Research*, Vol. 19, no. 3, pp. 185–186, 2008.

50. Lleo, A., E. Galea, and M. Sastre, "Molecular targets of non-steroidal anti-inflammatory drugs in neurodegenerative diseases," *Cellular and Molecular Life Sciences*, Vol. 64, pp. 1403–1418, June 2007.

51. Behl, C., J. Davis, G. M. Cole, and D. Schubert, "Vitamin E protects nerve cells from amyloid beta protein toxicity," *Biochemical and Biophysical Research Communications*, Vol. 86, no. 2, pp. 944–950, 1992.

52. Shah, S. A., G. H. Yoon, H.-O. Kim, and M. O. Kim, "Vitamin C Neuroprotection Against Dose-Dependent Glutamate-Induced Neurodegeneration in the Postnatal Brain," *Neurochemical Research*, Vol. 40, pp. 875–884, May 2015.

53. Kontush, A., and S. Schekatolina, "Vitamin E in Neurodegenerative Disorders: Alzheimer's Disease," *Annals of the New York Academy of Sciences*, Vol. 1031, pp. 249–262, Dec. 2004.

54. Spagnuolo, C., S. Moccia, and G. L. Russo, "Anti-inflammatory effects of flavonoids in neurodegenerative disorders," *European Journal of Medicinal Chemistry*, Vol. 153, pp. 105–115, June 2018.

55. Solanki, I., P. Parihar, M. L. Mansuri, and M. S. Parihar, "Flavonoid-Based Therapies in the Early Management of Neurodegenerative Diseases," *Advances in Nutrition*, Vol. 6, pp. 64–72, Jan. 2015.

56. Macready, A. L., O. B. Kennedy, J. A. Ellis, C. M. Williams, J. P. E. Spencer, and L. T. Butler, "Flavonoids and cognitive function: A review of human randomized controlled trial studies and recommendations for future studies," *Genes & Nutrition*, Vol. 4, pp. 227–242, Dec. 2009.

57. Güvenç, A., P. Houghton, H. Duman, M. Coşkun, and P. Şahin, "Antioxidant Activity Studies on Selected *Sideritis* . Species Native to Turkey," *Pharmaceutical Biology*, Vol. 43, pp. 173–177, Jan. 2005.

58. Güvenç, A., Y. Okada, E. K. Akkol, H. Duman, T. Okuyama, and İ. Çalış, "Investigations of anti-inflammatory, antinociceptive, antioxidant and aldose reductase inhibitory activities of phenolic compounds from Sideritis brevibracteata," *Food Chemistry*, Vol. 118, pp. 686–692, Feb. 2010.

59. Pérez-Hernández, J., V. J. Zaldívar-Machorro, D. Villanueva-Porras, E. Vega-Ávila, and A. Chavarría, "A Potential Alternative against Neurodegenerative Diseases: Phytodrugs," *Oxidative Medicine and Cellular Longevity*, Vol. 2016, pp. 1–19, 2016.

60. Akkentli, F., Y. P. Tan, and H. Saybasili, "Common Pesticide Rotenone Interference with Neuronal Transmission in Hippocampus," *American Journal of Biomedical Engineering*, Vol. 2, no. 6, pp. 212–217, 2012.

61. Mosmann, T., "Rapid colorimetric assay for cellular growth and survival: Application to proliferation and cytotoxicity assays," *Journal of Immunological Methods*, Vol. 65, pp. 55–63, Dec. 1983.

62. Bernas, T., and J. Dobrucki, "Mitochondrial and nonmitochondrial reduction of MTT: Interaction of MTT with TMRE, JC-1, and NAO mitochondrial fluorescent probes," *Cytometry*, Vol. 47, pp. 236–242, Apr. 2002.

63. Riccardi, C., and I. Nicoletti, "Analysis of apoptosis by propidium iodide staining and flow cytometry," *Nature Protocols*, Vol. 1, pp. 1458–1461, Aug. 2006.

64. Hamill, O. P., A. Marty, E. Neher, B. Sakmann, and F. J. Sigworth, "Improved patch-clamp techniques for high-resolution current recording from cells and cell-free membrane patches," *Pflügers Archiv - European Journal of Physiology*, Vol. 391, pp. 85–100, Aug. 1981.

65. Goldie, B. J., M. M. Barnett, and M. J. Cairns, "BDNF and the maturation of posttranscriptional regulatory networks in human SH-SY5Y neuroblast differentiation," *Frontiers in Cellular Neuroscience*, Vol. 8, Oct. 2014.

66. Xicoy, H., B. Wieringa, and G. J. Martens, "The SH-SY5Y cell line in Parkinson's disease research: A systematic review," *Molecular Neurodegeneration*, Vol. 12, pp. 1–11, Dec. 2017.

67. Fanger, G., J. Jones, and R. Maue, "Differential regulation of neuronal sodium channel expression by endogenous and exogenous tyrosine kinase receptors expressed in rat pheochromocytoma cells," *The Journal of Neuroscience*, Vol. 15, pp. 202–213, Jan. 1995.

68. Curci, A., F. Maqoud, A. Mele, M. Cetrone, M. Angelelli, N. Zizzo, and D. Tricarico, "Antiproliferative effects of neuroprotective drugs targeting big Ca2+-activated K+ (BK) channel in the undifferentiated neuroblastoma cells," *Current Topics in Pharmacology*, pp. 113–131, 2016.

69. Fell, S. M., S. Li, K. Wallis, A. Kock, O. Surova, V. Rraklli, C. S. Höfig, W. Li, J. Mittag, M. A. Henriksson, R. S. Kenchappa, J. Holmberg, P. Kogner, and S. Schlisio, "Neuroblast differentiation during development and in neuroblastoma requires KIF1Bβ-mediated transport of TRKA," *Genes & Development*, Vol. 31, pp. 1036–1053, May 2017.

70. Gudi, V., L. Gai, V. Herder, L. S. Tejedor, M. Kipp, S. Amor, K.-W. Sühs, F. Hansmann, A. Beineke, W. Baumgärtner, M. Stangel, and T. Skripuletz, "Synaptophysin Is a Reliable Marker for Axonal Damage," *Journal of Neuropathology & Experimental Neurology*, Vol. 76, pp. 109–125, Feb. 2017.

71. Miettinen, M., and J. Rapola, "Synaptophysin - An Immuno-histochemical Marker for Childhood Neuroblastoma," *Acta Pathologica Microbiologica Scandinavica Series C: Immunology*, Vol. 95A, pp. 167–170, 1987.

72. Fester, L., L. Zhou, A. Bütow, C. Huber, R. von Lossow, J. Prange-Kiel, H. Jarry, and G. M. Rune, "Cholesterol-promoted synaptogenesis requires the conversion of cholesterol to estradiol in the hippocampus," *Hippocampus*, Vol. 19, pp. 692–705, Aug. 2009.

73. Stone, D. J., I. Rozovsky, T. E. Morgan, C. P. Anderson, and C. E. Finch, "Increased Synaptic Sprouting in Response to Estrogen via an Apolipoprotein E-Dependent Mechanism: Implications for Alzheimer's Disease," *The Journal of Neuroscience*, Vol. 18, pp. 3180–3185, May 1998.

74. Clay, J., "Comparison of the effects of internal TEA+ and Cs+ on potassium current in squid giant axons," *Biophysical Journal*, Vol. 48, pp. 885–892, Dec. 1985.

75. Toselli, M., P. Tosetti, and V. Taglietti, "Functional changes in sodium conductances in the human neuroblastoma cell line SH-SY5Y during in vitro differentiation," *Journal of Neurophysiology*, Vol. 76, pp. 3920–3927, Dec. 1996.

76. Mustata, M., K. Ritchie, and H. A. McNally, "Neuronal elasticity as measured by atomic force microscopy," *Journal of Neuroscience Methods*, Vol. 186, pp. 35–41, Jan. 2010.

77. Lekka, M., "Discrimination Between Normal and Cancerous Cells Using AFM," *BioNanoScience*, Vol. 6, pp. 65–80, Mar. 2016.